

1 **Effects of fluctuating hypoxia on benthic oxygen**  
2 **consumption in the Black Sea (Crimean Shelf)**

3

4 **A. Lichtschlag<sup>1, +</sup>, D. Donis<sup>1, ++</sup>, F. Janssen<sup>1, 2</sup>, G. L. Jessen<sup>1</sup>, M. Holtappels<sup>1, 3</sup>, F.**  
5 **Wenzhöfer<sup>1, 2</sup>, S. Mazlumyan<sup>4, +++</sup>, N. Sergeeva<sup>4, ++++</sup>, C. Waldmann<sup>3</sup>, A. Boetius<sup>1, 2</sup>**

6 [1] {Max Planck Institute for Marine Microbiology, Celsiusstrasse 1, 28359 Bremen,  
7 Germany}

8 [2] {HGF MPG Research Group for Deep Sea Ecology and Technology, Alfred Wegener  
9 Institute for Polar and Marine Research, Am Handelshafen, 27515 Bremerhaven, Germany}

10 [3] {MARUM – Center for Marine Environmental Sciences, University of Bremen, 28334  
11 Bremen, Germany}

12 [4] {A.O. Kovalevsky Institute of Biology of Southern Seas, 2, Nakhimov ave., Sevastopol,  
13 299011}

14 [+] current address: National Oceanography Center, University of Southampton Waterfront  
15 Campus, European Way, SO14 3ZH, Southampton, UK}

16 [++] current address: F.-A. Forel Institute, University of Geneva, Batelle, Bat. D, 7 Route de  
17 Drize- 1227 Carouge, Geneva, Switzerland}

18 [+++] current address: Institute of Natural & Technical Systems Russian Academy of  
19 Sciences, Lenin St.28, Sevastopol, 29901, [xn--h1aogd.xn--p1ai](http://xn--h1aogd.xn--p1ai)

20 [++++] current address: The A.O. Kovalevsky Institute of Marine Biological Research of  
21 RAS, 119000, Moscow, Leninsky Ave., 32, [imbr.iuf.net](http://imbr.iuf.net)

22 Correspondence to: Anna Lichtschlag ([alic@noc.ac.uk](mailto:alic@noc.ac.uk))

23

24 **Abstract**

25 The outer Western Crimean Shelf of the Black Sea is a natural laboratory to investigate  
26 effects of stable oxic versus varying hypoxic conditions on seafloor biogeochemical processes  
27 and benthic community structure. Bottom water oxygen concentrations ranged from normoxic  
28 ( $175 \mu\text{mol O}_2 \text{ L}^{-1}$ ) and hypoxic ( $< 63 \mu\text{mol O}_2 \text{ L}^{-1}$ ) or even anoxic/sulfidic conditions within a  
29 few kilometres distance. Variations in oxygen concentrations between  $160$  and  $10 \mu\text{mol L}^{-1}$

1 even occurred within hours close to the chemocline at 134 m water depth. Total oxygen  
2 uptake, including diffusive as well as fauna-mediated oxygen consumption, decreased from on  
3 average  $15 \text{ mmol m}^{-2} \text{ d}^{-1}$  in the oxic zone to on average  $7 \text{ mmol m}^{-2} \text{ d}^{-1}$  in the hypoxic zone,  
4 correlating with changes in macrobenthos composition. Benthic diffusive oxygen uptake  
5 rates, comprising respiration of microorganisms and small meiofauna, were similar in oxic  
6 and hypoxic zones (on average  $4.5 \text{ mmol m}^{-2} \text{ d}^{-1}$ ), but declined to  $1.3 \text{ mmol m}^{-2} \text{ d}^{-1}$  in bottom  
7 waters with oxygen concentrations below  $20 \mu\text{mol L}^{-1}$ . Measurements and modelling of pore  
8 water profiles indicated that reoxidation of reduced compounds played only a minor role in  
9 diffusive oxygen uptake under the different oxygen conditions, leaving the major fraction to  
10 aerobic degradation of organic carbon. Remineralization efficiency decreased from nearly  
11 100% in the oxic zone, to 50 % in the oxic-hypoxic, to 10 % in the hypoxic-anoxic zone.  
12 Overall the faunal remineralization rate was more important, but also more influenced by  
13 fluctuating oxygen concentrations, than microbial and geochemical oxidation processes.

14

## 15 **1 Introduction**

16 Hypoxia describes a state of aquatic ecosystems in which low oxygen concentrations affect  
17 the physiology, composition and abundance of fauna, consequently altering ecosystem  
18 functions including biogeochemical processes and sediment-water exchange rates  
19 (Middelburg and Levin, 2009). Low faunal bioturbation rates in hypoxic zones limit sediment  
20 ventilation (Glud, 2008), decreasing oxygen availability for aerobic respiration. Hence,  
21 sediments underlying a low oxygen water column often show oxygen penetration depths of  
22 only a few millimeters (Archer and Devol, 1992; Glud et al., 2003; Rasmussen and Jørgensen,  
23 1992). This increases the contribution of anaerobic microbial metabolism to organic matter  
24 remineralization at the expense of aerobic degradation by microbes and fauna as reported  
25 from the Romanian Shelf area of the Black Sea (Thamdrup et al., 2000; Weber et al., 2001),  
26 the Neuse River Estuary (Baird et al., 2004), and the Kattegat (Pearson and Rosenberg, 1992).  
27 Consequently, oxygen is channeled into the reoxidation of reduced substances produced  
28 during anaerobic degradation of organic matter and lost for direct aerobic respiration. Even  
29 temporarily reduced bottom water oxygen concentrations can repress seafloor oxygen uptake  
30 that should become enhanced by algae blooms and temperature increases (Rasmussen and  
31 Jørgensen, 1992). However, depending on frequency and duration of oxygen oscillations,  
32 oxygen consumption following an anoxic event can also be significantly increased (Abril et

1 al., 2010). Hence, these and other studies have indicated, that not only the degree of  
2 oxygenation plays an important role in oxygen uptake, but also the frequency and persistency  
3 of the low oxygen conditions can shape faunal activity, biogeochemical processes, and the  
4 functioning of the ecosystem as a whole (Boesch and Rabalais, 1991, Diaz, 2001, Friedrich et  
5 al., 2014).

6 The outer Western Crimean Shelf of the Black Sea is a natural laboratory where long-term  
7 effects of different, and locally fluctuating oxygen concentrations on benthic oxygen  
8 consumption and biogeochemical processes can be investigated, which was the main aim of  
9 this study. In the Black Sea, the depth of the oxic-anoxic interface changes from about 70-100  
10 m in open waters (Friedrich et al., 2014) to depths of > 150 m above the shelf break (Stanev et  
11 al., 2013). This interface is stabilized by a halocline that separates the upper layer of brackish,  
12 oxic water (salinity < 17) from the saline, anoxic and sulfidic deep waters below (Tolmazin,  
13 1985). Due to mixing processes by internal waves and eddies, the location of this interface  
14 zone is more dynamic along the margins of the Black Sea compared to the open sea. In the  
15 shelf region, hypoxic waters with oxygen concentrations < 63  $\mu\text{mol L}^{-1}$  oscillate over > 70 m  
16 in water depth on time scales of hours to months (Stanev et al., 2013). On the outer Western  
17 Crimean Shelf, such strong vertical fluctuations affect a 40 km wide area of the slope  
18 (Friedrich et al., 2014; Luth et al., 1998). Consequences of fluctuating hypoxia on benthic  
19 community structure is known from other areas on the Black Sea shelf with seasonally  
20 hypoxic coastal areas with water stagnation and high organic carbon accumulation (Zaika et  
21 al., 2011).

22 Here we investigated biogeochemical processes on the outer Western Crimean Shelf to assess  
23 how different ranges of oxygen availability, and also of fluctuations in bottom water oxygen  
24 concentrations, influence respiration, organic matter remineralization and the distribution of  
25 benthic organisms. The questions addressed are to what extent the variability in oxygen  
26 concentration has an effect on (1) the remineralization rates, (2) the proportion of microbial vs.  
27 fauna-mediated respiration, (3) the community structure and (4) the share of anaerobic vs.  
28 aerobic microbial respiration pathways.

29

## 30 **2 Methods**

## 1 **2.1 Study site on the outer Western Crimean Shelf**

2 Investigations of bottom water oxygen concentrations and biogeochemistry of the underlying  
3 seafloor of the outer Western Crimean Shelf were carried out over a time period of 2 weeks  
4 (20<sup>th</sup> April - 7<sup>th</sup> May 2010) during leg MSM 15/1 of R/V Maria S. Merian. The selected area  
5 on the outer shelf has a gentle slope and a maximum width of around 60 km until the shelf  
6 break at approx. 200 m water depth. The sediment and the water column were sampled along  
7 a transect from 95 m to 218 m water depth within an area of about 100 km<sup>2</sup> (Fig. 1). Detailed  
8 information of all stations in the working area is given in Table 1. All biogeochemical data are  
9 deposited in the Earth System database [www.PANGAEA.de](http://www.PANGAEA.de) and are available at  
10 <http://dx.doi.org/10.1594/PANGAEA.844879>.

## 11 **2.2 Water column CTD and oxygen measurements**

12 Bottom water oxygen concentrations were recorded repeatedly between 95 m to 218 m water  
13 depth at different spatial and temporal scales with various sensors, which were all calibrated  
14 by Winkler titration (Winkler, 1888). A total of 26 casts were performed with a CTD/Rosette  
15 equipped with a SBE 43 oxygen sensor (Seabird Electronics, Bellevue, WA, USA). A  
16 mooring was deployed at 135 m water depth 1.5 m above the sediment, equipped with a  
17 Seaguard current meter with CTD and a type 4330 oxygen optode (Aanderaa Data  
18 Instruments, Bergen, Norway) recording at 60 seconds intervals at a distance of 1.5 m above  
19 the sediment from the 30<sup>th</sup> April to the 7<sup>th</sup> May 2010. A second mooring was deployed for the  
20 same time period at 100 m water depth, with a CTD attached at 1.5 meter above the sediment  
21 (type SBE 16, Seabird Electronics) to record density, salinity and temperature. CTD water  
22 column casts and the mooring at 135 m showed that oxygen concentrations strongly correlate  
23 with density ( $R^2 = 0.997$ ). Hence, oxygen concentrations at the 100 m mooring site were  
24 calculated from the density recordings at this site using a density-oxygen relationship (4<sup>th</sup>  
25 order polynomial fit) based on the compiled mooring/CTD data. Additionally, bottom water  
26 oxygen concentration was measured at the seafloor by oxygen optodes mounted on the  
27 manned submersible JAGO (GEOMAR, Kiel; Aanderaa optode type 3830), and to a Benthic  
28 Boundary Layer-Profiler (Holtappels et al., 2011) (Aanderaa optode type 4330). Furthermore,  
29 microprofilers equipped with oxygen microsensors were mounted on a lander and a crawler  
30 (see 2.5.1). For consistency with other hypoxia studies, we use the oxygen threshold of 63  
31  $\mu\text{mol L}^{-1}$  as upper boundary for hypoxia (Diaz, 2001). Sulfide concentrations were determined  
32 in bottom water collected with Niskin bottles during CTD casts and JAGO dives at 13

1 different locations between 135 m and 218 m water depth. For all water column oxygen and  
2 sulfide concentrations a limit of  $2 \mu\text{mol L}^{-1}$  was defined, below which concentrations were  
3 assumed to be zero.

### 4 **2.3 Visual seafloor observations and micro-topography scans**

5 To observe organisms, their traces of life, and the resulting micro-topography at the surface of  
6 the different seafloor habitats, a laser scanning device (LS) and the high-resolution camera  
7 MEGACAM were used on the benthic crawler MOVE (MARUM, Bremen). The LS consisted  
8 of a linear drive that moved a downward looking line laser together with a monochrome  
9 digital camera horizontally along a 700 mm long stretch of the seafloor. The position of the  
10 approx. 200 mm wide laser line was recorded by the camera from an angle of  $45^\circ$  and the 3-D  
11 micro-topography of the scanned area was determined on a  $1 \times 1 \text{ mm}^2$  horizontal grid at sub-  
12 mm accuracy (for a detailed description see Cook et al., 2007). The roughness of the sediment  
13 surface was quantified in three 700 mm long profiles extracted from the sides and along the  
14 center line of 7, 2, 6, and 2 micro-topographies scanned at 104, 138, 155, and 206 m water  
15 depth, respectively. Roughness was determined for different length scales by calculating mean  
16 absolute vertical differences to the same profile previously smoothed by applying moving  
17 average with 3 to 300 mm averaging window size.

18 The downward-looking MEGACAM (Canon EOS T1i with 15 megapixel imager and 20 mm  
19 wide-angle lens) was either attached directly to MOVE or added to the horizontal drive of the  
20 LS; the latter configuration facilitating imaging of larger sediment stretches by photo-  
21 mosaicking. In addition, visual seafloor observations were carried out before pushcore  
22 sampling by JAGO. Dive videos were recorded with a type HVR-V1E HDV Camcorder  
23 (SONY, Tokyo, Japan) mounted in the center of JAGO's large front viewport during 19 dives.  
24 During each dive, video still images were captured by video-grabber from the running camera.

### 25 **2.4 Faunal analyses**

26 Meiofauna organisms were studied in the upper 5 cm sediment horizons of 2-4 cores per  
27 station, with each core covering an area of  $70.9 \text{ cm}^2$  (TVMUC) and  $41.8 \text{ cm}^2$  (for JAGO  
28 pushcore) (Table 1, Fig. 1). The abundances were extrapolated to  $\text{m}^2$ . Sediments were washed  
29 with filtered or distilled water through sieves with mesh sizes of 1 mm and  $63 \mu\text{m}$ , and  
30 preserved in 75 % alcohol to conserve the morphological structures of the meiofauna.  
31 Subsequently, samples were stained with Rose Bengal, to separate living and dead / decaying

1 organisms (Grego et al., 2013), and sorted in water using a binocular (x 90 magnification) and  
2 a microscope (Olympus CX41 using different magnifications up to x 1000). Only organisms  
3 that strongly stained with Rose Bengal and showed no signs of morphological damage were  
4 considered as being alive at the time of sampling. All of the isolated organisms were counted  
5 and identified to higher taxa. In the same cores we analyzed fauna that are larger than 1.5-2.0  
6 mm and that from their size are representatives of macrobenthos. Also this share of fauna was  
7 identified to higher taxa under the microscope, counted and the abundances extrapolated to m<sup>2</sup>.  
8 Statistical analyses of the similarity of meiofauna communities were conducted using the R  
9 package vegan (Oksanen et al., 2010) and performed in R (v. 3.0.1; <http://www.R-project.org>).  
10 Richness was calculated from species (taxa) presence/absence. A matrix based on Bray-Curtis  
11 dissimilarities was constructed from the Hellinger-transformed abundances for meiofauna  
12 taxa. The non-parametric Analysis of Similarity (ANOSIM) was carried out to test whether  
13 the communities (based on different bottom-oxygen zones) were significantly different  
14 (Clarke 1993).

## 15 **2.5 Benthic exchange rates**

### 16 **2.5.1 In situ microsensor measurements**

17 Vertical solute distributions were measured in situ at high resolution in sediment pore waters  
18 and the overlying waters with microsensors mounted on microprofiler units (Boetius and  
19 Wenzhöfer, 2009). In particular, Clark-type O<sub>2</sub> microsensors (Revsbech, 1989) and H<sub>2</sub>S  
20 microsensors (Jeroschewski et al., 1996) were used as well as microsensors for pH - either  
21 LIX-type (de Beer et al., 1997) or needle-type (type MI 408, Microelectrodes Inc., Bedford,  
22 NH, USA). A two-point oxygen sensor calibration was done in situ, using water column  
23 oxygen concentrations obtained from simultaneous oxygen recordings and zero readings in  
24 anoxic sediment layers. The H<sub>2</sub>S sensors were calibrated at in situ temperature on board at  
25 stepwise increasing H<sub>2</sub>S concentrations by adding aliquots of a 0.1 mol L<sup>-1</sup> Na<sub>2</sub>S solution to  
26 acidified seawater (pH <2). pH sensors were calibrated with commercial laboratory buffers  
27 and corrected with pH obtained from water samples taken with Niskin bottles operated by  
28 JAGO.

29 Profiler units were mounted either on the benthic crawler MOVE (Waldmann and Bergenthal,  
30 2010) or on a benthic lander (Wenzhöfer and Glud, 2002). The MOVE vehicle was connected  
31 to the ship via a fiber optic cable that allowed continuous access to video and sensor data. The  
32 maneuverability of the vehicle allowed targeting spots of interest on the seafloor in the cm

1 range. The profiler units were equipped with 3-4 O<sub>2</sub> microsensors, 2 H<sub>2</sub>S microsensors, and 1-  
2 2 pH sensors. Microprofiles across the sediment-water interface were performed at a vertical  
3 resolution of 100 μm and had a total length of up to 18 cm. During each deployment of the  
4 lander the microsensor array performed up to three sets of vertical profiles at different  
5 horizontal positions, each 26 cm apart.

6 From the obtained oxygen profiles the diffusive oxygen uptake (DOU) was calculated based  
7 on the gradients in the diffusive boundary layer (DBL) according to Fick's first law of  
8 diffusion,

$$9 \quad J = \frac{dc}{dx} \times D_0 \quad (1)$$

10 where J is the oxygen flux, dc/dx is the concentration gradient, and D<sub>0</sub> is the diffusion  
11 coefficient of oxygen in water (D<sub>0</sub>O<sub>2</sub> = 1.22 x 10<sup>-4</sup> m<sup>2</sup> d<sup>-1</sup>, Broecker and Peng (1974)) at the  
12 ambient temperature (8 °C) and salinity (18-20). For each station, selected oxygen profiles  
13 were fitted using the software PROFILE (Berg et al., 1998) to determine oxygen consumption  
14 from the shape of the pore water gradient and to identify depth intervals of similar oxygen  
15 consumption based on statistical F-testing.

## 16 **2.5.2 In situ benthic chamber incubations**

17 Total oxygen uptake (TOU) of sediments was measured by in situ benthic chamber  
18 incubations using 2 platforms: (1) Two benthic chambers, each integrating an area of 0.2 ×  
19 0.2 m (Witte and Pfannkuche, 2000) mounted to the same benthic lander frame used for  
20 microprofiler measurements (Wenzhöfer and Glud, 2002) and (2) a circular chamber (r =  
21 0.095 m, area = 0.029 m<sup>2</sup>) attached to the benthic crawler MOVE for video-guided chamber  
22 incubations. After positioning MOVE at the target area the chamber was lowered into the  
23 sediment, controlled by the video camera of MOVE and operated online through the MOVE-  
24 electronics. Both systems were equipped with a stirrer and syringe samplers that took up to 6  
25 successive samples (V = 50 mL) from the 0.1-0.15 m high overlying bottom water. Benthic  
26 exchange rates were determined from the linear regression of oxygen solute concentration  
27 over time inside the enclosed water body that was continuously monitored for a period of 2 to  
28 4 h by 1 or 2 oxygen optodes mounted in the chamber lid. The optodes were calibrated with a  
29 zero reading at in situ temperature on board and with bottom water samples, in which  
30 concentrations were determined either by Winkler titration (Winkler, 1888) or with a  
31 calibrated Aanderaa optode attached to the outside of the chamber. At the beginning of the  
32 incubation period, oxygen concentrations in the chamber were the same as in situ bottom

1 water concentrations outside the chamber. Only during deployments in the hypoxic-anoxic  
2 zone, oxygen concentrations in the chambers were higher than in the surrounding bottom  
3 water, due to enclosure of oxygen-rich water during descent. These measurements were used  
4 to estimate potential TOU rates at intermittently higher oxygen concentration. To estimate the  
5 in situ TOU/DOU ratio for the hypoxic-anoxic zone, in this case we modeled the DOU at  
6 these specific conditions based on the volumetric rate and the DBL thickness determined by  
7 the in situ microsensor profile.

## 8 **2.6 Geochemical analyses of the sediments and sulfate reduction rates**

9 Sediments for geochemical analyses were sampled with a video-guided multicorer (TVMUC)  
10 at 4 stations between 104 and 207 m (Table 1). Pore water was extracted from sediment cores  
11 within 3 h after retrieval in 1 cm (upper 5 cm) or 2 cm (> 5 cm) intervals with Rhizons (type:  
12 CSS, Rhizosphere Research Products, pore size < 0.2  $\mu\text{m}$ , length 5 cm) at in situ temperature  
13 (8  $^{\circ}\text{C}$ ) in a temperature-controlled room. To extract sufficient amounts of pore water two  
14 Rhizons were inserted horizontally at each depth interval in holes that were drilled at the  
15 same depth, with a 90 $^{\circ}$  angle. Using this procedure, the amount of pore water removed per  
16 Rhizon was less than 4 mL and mixing of pore water across the different horizons was  
17 avoided (Seeberg-Elverfeldt et al., 2005). Samples were fixed for Fe (II), Mn (II), sulfide and  
18 sulfate analyses as described in Lichtschlag et al. (2010). For ammonium and nitrate analyses  
19 samples were frozen at -20  $^{\circ}\text{C}$ . In addition, one sediment core from each station was sliced in  
20 1 cm intervals (upper 10 cm) and 2 cm intervals (>10 cm depth) for solid phase analyses.  
21 Aliquots were stored at 4  $^{\circ}\text{C}$  for porosity analyses and frozen at -20  $^{\circ}\text{C}$  for  $^{210}\text{Pb}$  and solid  
22 phase iron, manganese and elemental sulfur analyses.

23 Pore water constituents were analyzed by the following procedures: Dissolved Mn (II) and Fe  
24 (II) were measured with a Perkin Elmer 3110 flame atomic absorption spectrophotometer  
25 (AAS) with a detection limit of 5  $\mu\text{mol L}^{-1}$  for iron and manganese. Total sulfide  
26 concentrations ( $\text{H}_2\text{S} + \text{HS}^- + \text{S}^{2-}$ ) were determined with the diamine complexation method  
27 (Cline, 1969). A Skalar Continuous-Flow Analyzer was used for ammonium and nitrate  
28 analyses following the procedures described in Grasshoff (1983), with a detection limit of 1  
29  $\mu\text{mol L}^{-1}$ . Sulfate concentrations in pore water were determined by non-suppressed anion  
30 exchange chromatography (Metrohm 761 Compact IC) after filtration and dilution. To  
31 determine fluxes of iron, manganese, sulfide and ammonium the pore water profiles were  
32 fitted using the software PROFILE (Berg et al., 1998).



1 Total zero-valent sulfur in sediments was extracted with methanol from sediment preserved in  
2 ZnAc (Zopfi et al., 2004) and analyzed by HPLC. Concentrations of acid volatile sulfide  
3 (AVS =  $\text{Fe}_3\text{S}_4$ ,  $\text{FeS}$ ) and chromium reducible sulfur (CRS =  $\text{FeS}_2$ , some  $\text{S}^0$ , remaining  $\text{Fe}_3\text{S}_4$ )  
4 were determined on frozen sediment aliquots by the two-step Cr-II distillation method  
5 (Fossing and Jørgensen, 1989). Solid phase reactive iron and manganese were extracted from  
6 frozen sediments after the procedure of Poulton and Canfield (2005) using sequentially Na-  
7 acetate, hydroxylamine-HCl, dithionite and oxalate. Manganese and iron concentrations were  
8 measured as described above. Organic carbon content in the first cm of the sediments was  
9 determined on freeze-dried and homogenized samples and measured using a Fisons NA-1500  
10 elemental analyzer.

11 Sulfate reduction rates were determined with the whole core incubation method described in  
12 Jørgensen (1978). On board 10  $\mu\text{L}$  aliquots of an aqueous  $^{35}\text{SO}_4^{2-}$  tracer solution (activity 11.5  
13  $\text{kBq } \mu\text{L}^{-1}$ ) were injected into the sediments in 1 cm intervals and samples were incubated for  
14 up to 24 h at in situ temperature, until the sediments were sliced into 20 mL 20 % ZnAc.  
15 Tracer turnover rates were determined with the single-step cold distillation method  
16 (Kallmeyer et al., 2004). Three replicates were measured per station and results were  
17 integrated over the upper 10 cm of the sediment.

18 Porosity and solid-phase density were determined by drying a wet sediment aliquot of known  
19 volume at 105 °C until constant weight and weighing before and after.

20 Sedimentation rates were determined from excess  $^{210}\text{Pb}$  activity ( $^{210}\text{Pb}_{\text{xs}}$ ) in frozen sediment  
21 aliquots of the upper 10 cm that were freeze-dried and homogenized by grinding. Activities of  
22  $^{210}\text{Pb}$ ,  $^{214}\text{Pb}$  and  $^{214}\text{Bi}$  were determined on 5-30 g aliquots by non-destructive gamma  
23 spectrometry using an ultra-low-level germanium gamma detector (EURISYS coaxial type N,  
24 Canberra Industries, Meriden, CT, U.S.A.). Sediment accumulation rates ( $\text{g cm}^{-2} \text{ yr}^{-1}$ ) were  
25 calculated from the undisturbed part of the sediments from the change of the unsupported  
26  $^{210}\text{Pb}_{\text{xs}}$  activity with sediment accumulation, expressed as cumulative dry weight ( $\text{g cm}^{-2}$ ) and  
27 using the calculations described by Niggemann et al. (2007). This calculation is based on the  
28 assumption that the  $^{210}\text{Pb}_{\text{xs}}$  flux and sedimentation were constant over time.

29

## 1 **3 Results**

### 2 **3.1 Oxygen regime of the outer Western Crimean Shelf**

3 Recordings of bottom water oxygen concentrations (n=85) along the transect from 95 m to  
4 218 m water depth served to differentiate four zones of different bottom water oxygenation  
5 within a distance of more than 30 km (Table 1; Fig. 1; Fig. 2):

6 The “oxic zone” at water depths of 95 to 130 m had oxygen concentrations of on average 116  
7  $\pm 29 \mu\text{mol L}^{-1}$  (31 % air saturation at ambient conditions; 8 °C, salinity of 19), and remained  
8 above the threshold for hypoxia ( $63 \mu\text{mol L}^{-1}$ ) throughout the period of our observations.  
9 Recordings from the mooring at 100 m water depth showed some fluctuations (Fig. S1a in the  
10 Supplement), with oxygen concentrations varying between 100 - 160  $\mu\text{mol L}^{-1}$  within 6 days.  
11 In this oxic zone, sediment surface color was brownish, and the seafloor looked rather  
12 homogenous, without ripple structures, but with faunal traces (Fig. S2a). The top 5 cm of the  
13 sediment comprised some shell debris of 2 - 6 mm diameter encrusted with a bright orange  
14 layer of up to 3 mm thickness, which most probably consisted of iron-oxides (Fig. S2b).  
15 During JAGO dives and MOVE deployments we recorded living fauna in the oxic zone such  
16 as clams, ascidians, phoronids, cerianthids, porifera and many fish (Fig. S2c). Traces of recent  
17 faunal activity at the seafloor included trails, worm borrows and feces (Fig. S2a). During our  
18 sampling campaign the horizontal distance to the oxic-anoxic interface (chemocline) was on  
19 average 13 km. The oxic zone served as reference for further comparisons of hypoxic effects  
20 on biogeochemical processes and faunal community composition.

21 In the “oxic-hypoxic zone” at water depths between 130 m to 142 m, average bottom water  
22 oxygen concentrations were  $94 \pm 56 \mu\text{mol L}^{-1}$  (approx. 25 % air saturation at ambient  
23 conditions; 8 °C, salinity of 20). However, we observed strong variations in oxygen  
24 concentrations with maxima of up to  $176 \mu\text{mol L}^{-1}$  and minima of  $9 \mu\text{mol L}^{-1}$ , respectively.  
25 Hypoxic conditions prevailed for 30 % of the observation period of 7 days, as recorded by the  
26 stationary mooring at 135 m water depth (Fig. S1b). Constantly rising oxygen concentrations  
27 over days were interspersed by a substantial drop from fully oxic to almost anoxic conditions  
28 within < 3 h (Fig. S1b). Horizontal distance to the oxic-anoxic interface was on average 7 km  
29 during our expedition. In the oxic-hypoxic zone, only few fishes were observed, and video-  
30 observations of the seafloor showed a clear reduction of epibenthos abundance and their  
31 traces compared to those in the oxic zone.

1 The “hypoxic-anoxic” zone between 142 and 167 m water depth sediments showed  
2 fluctuating hypoxic conditions between 0 - 63  $\mu\text{mol L}^{-1}$  (average  $11 \pm 16 \mu\text{mol L}^{-1}$ ; 3 % air  
3 saturation at ambient conditions; 8 °C, salinity of 20). Unexpectedly, during a short period at  
4 these water depths, some fish (the sprattus *Sprattus phalericus* at 145 and 163 m water depth,  
5 and the whiting *Merlangius merlangus euxinus* at 145 m water depth, Zaika and Gulin (2011))  
6 were observed when oxygen concentrations were as low as 20  $\mu\text{mol L}^{-1}$  (Fig. S2f). The  
7 seafloor was covered with fluffy greenish-brownish material and sediments showed a fine  
8 lamination (Fig. S2e). No epibenthic life was observed, nor borrows or other traces of bottom  
9 dwelling fauna.

10 Below 167 m, the bottom water was permanently anoxic during the time period of our  
11 campaign. Below 180 m sulfide was constantly present in the bottom water, with  
12 concentrations ranging between 5-23  $\mu\text{mol L}^{-1}$  (Fig. 2). In this “anoxic-sulfidic” zone  
13 sediments were dark green-blackish. Neither macrofauna, nor traces of bottom-dwelling  
14 infauna were observed.

### 15 **3.2 Meiofauna composition and abundance**

16 Abundance and composition of meiobenthos as retrieved from the top 5 cm of pooled core  
17 samples are compared across the different zones of oxygen availability in Figure 6 and Table  
18 S2 in the Supplement. The macrobenthos abundances and taxonomic composition presented  
19 here are not quantitative, nor statistically significant, for the entire size class due to the limited  
20 sample size available; they might represent mostly small types and juvenile stages (Table S1  
21 in the Supplement). These decreased by more than one order of magnitude from the oxic zone  
22 ( $21 \times 10^3$  individuals  $\text{m}^{-2}$ ) to the hypoxic-anoxic zone ( $1 \times 10^3$  individuals  $\text{m}^{-2}$ ) (Table S1). In  
23 the oxic zone, cnidaria dominated the benthic community next to oligochaetes and  
24 polychaetes, also bivalves and gastropods were present. A peak in macrobenthos abundances  
25 in both the oxic and the oxic-hypoxic zone at around 129-138 m was related to an  
26 accumulation of cnidarians with abundances of up to  $54 \times 10^3$  individuals  $\text{m}^{-2}$  (Table S1). Also  
27 the two hypoxic zones were dominated by cnidaria. In accordance with the results from  
28 sampling, no larger macrofauna was documented during JAGO dives in these zones.

29 Meiobenthos was composed of similar groups and abundances in the oxic and oxic-hypoxic  
30 zone with densities of around  $200 \times 10^4$  individuals  $\text{m}^{-2}$  (Fig. 3, Table S2). A substantial  
31 decrease to  $50 \times 10^4$  individuals  $\text{m}^{-2}$  was observed between these two zones and the hypoxic-  
32 anoxic zone. The meiofaunal community structure changed according to the oxygenation

1 regime (Fig. 4), showing significant differences between oxic and hypoxic-anoxic zones  
2 (ANOSIM-R = 0.7, Bonferroni corrected P value < 0.05) together with the highest  
3 dissimilarities (up to 50%, Table S3). Nematodes dominated meiofauna composition in all  
4 oxic and hypoxic zones (Table S2). In the oxic zone ostracodes were the 2<sup>nd</sup> most abundant  
5 species. These were replaced by benthic foraminifera in the oxic-hypoxic and the hypoxic-  
6 anoxic zone. Altogether meiofaunal richness (taxa count, average  $\pm$ SD) was similar in the  
7 oxic zone and oxic-hypoxic zone ( $15 \pm 2$  and  $15 \pm 1$ ) and dropped to  $9 \pm 1$  in the hypoxic-  
8 anoxic zone.

### 9 **3.3 Benthic oxygen fluxes and respiration rates**

10 A total of 33 oxygen microprofiles were measured during seven deployments of the benthic  
11 crawler MOVE and the lander at water depths between 104 and 155 m. Oxygen penetration  
12 depths and dissolved oxygen uptake rates are summarized in Table 2. The shape of the  
13 profiles and the differences in oxygen penetration depth as shown in Figure 5 reflect the  
14 spatial variations of oxygen bottom water concentrations and oxygen consumption rates. In  
15 the shallowest, oxic zone (104 m) clear signs of bioturbation were visible from the irregular  
16 shape of about 25 % of the profiles, occasionally increasing the oxygen penetration depth up  
17 to approximately 10 mm. Bioturbation activity was in accordance with a significant  
18 bioturbated surface layer and more pronounced roughness elements at the sediment surface at  
19 the shallowest site as compared to deeper waters (see section 3.5). In contrast, the shape of the  
20 oxygen profiles obtained in the oxic-hypoxic and the hypoxic-anoxic zone showed no signs of  
21 bioturbation. Small-scale spatial heterogeneity was low between parallel sensor measurements  
22 and within one deployment (area of  $176 \text{ cm}^2$  sampled). However, strong temporal variations  
23 occurred in response to the fluctuations in bottom water oxygen concentration. For example,  
24 in the oxic-hypoxic zone a clear relation between oxygen penetration depth and bottom water  
25 oxygen concentration was detectable, with increased bottom water oxygen concentration  
26 leading to deeper oxygen penetration depth (Fig. 5 a-c). Except where bioturbation led to  
27 slightly deeper penetration, oxygen was depleted within the first 0.4-3 mm of the surface layer  
28 (Fig. 5, Table 2).

29 Diffusive oxygen uptake (DOU) ranged within an order of magnitude between all zones  
30 (Table 2). The highest DOU of  $8.1 \text{ mmol m}^{-2} \text{ d}^{-1}$  was calculated from a profile obtained at 104  
31 m water depth in the oxic zone, but the averages of all oxygen fluxes measured in the oxic and  
32 oxic-hypoxic zones were similar (averages  $\pm$ SD of  $4.6 \pm 1.8 \text{ mmol m}^{-2} \text{ d}^{-1}$  and  $4.4 \pm 1.9$ ,

1 respectively, Table 2). The higher variability within the oxic-hypoxic zone, spanning from 0.6  
2 to 8 mmol m<sup>-2</sup> d<sup>-1</sup> between measurements, matches the higher variability in bottom water  
3 oxygen concentrations observed for this zone (Fig. 4b). Diffusive oxygen uptake in that zone  
4 was lowest after a nearly anoxic event (~10 μmol O<sub>2</sub> L<sup>-1</sup>; Fig. S1b). However, highest fluxes  
5 in the oxic-hypoxic zone were not recorded during a “normoxic event” (144 μmol O<sub>2</sub> L<sup>-1</sup>, Fig.  
6 5b), but at the typical intermediate bottom water oxygen concentration of approx. 90 μmol L<sup>-1</sup>  
7 (Station 434; Fig. 5c, Fig. S1b). In the hypoxic-anoxic zone DOU was only 25% of that in the  
8 oxic and oxic-hypoxic zones (average: 1.3 ±0.5 mmol m<sup>-2</sup> d<sup>-1</sup>).

9 In bottom waters of the hypoxic-anoxic zone high resolution measurements of pH indicated a  
10 pH of around 7.8, decreasing to values between 7.2 - 7.4 in the sediment. With the H<sub>2</sub>S  
11 microsensors no free sulfide was detected in the pore waters of the oxic, oxic-hypoxic or  
12 hypoxic-anoxic zones down to the measured depth of 15 cm in the sediment. In the anoxic-  
13 sulfidic zone the microsensor measurements failed. Bottom water sulfide concentrations were  
14 > 5 μmol L<sup>-1</sup>, and the pore water analyses indicated high concentrations of sulfide of up to  
15 1000 μmol L<sup>-1</sup> in the sediment (see 3.4).

16 Total oxygen uptake (TOU) including the faunal respiration, was generally higher than DOU  
17 (Table 2). Individual measurements varied from 20.6 to 3.2 mmol m<sup>-2</sup> d<sup>-1</sup> across all zones.  
18 Average TOU showed a clear reduction from the oxic zone (average: 14.9 ±5.1 mmol m<sup>-2</sup> d<sup>-1</sup>)  
19 to the oxic-hypoxic zone (average: 7.3 ±3.5 mmol m<sup>-2</sup> d<sup>-1</sup>). TOU at the oxic-hypoxic station  
20 compare well with a TOU of 6.0 and 4.2 mmol m<sup>-2</sup> d<sup>-1</sup> determined by simultaneous eddy  
21 correlation measurements averaged over a time period of 14 hours (Holtappels et al., 2013).

22 Trapping of oxygen-enriched waters in the chambers during deployments carried out at the  
23 hypoxic-anoxic zone led to higher initial oxygen concentrations in the enclosed water as  
24 compared to ambient bottom waters. Therefore, we could only obtain potential TOU rates at  
25 elevated bottom water concentrations of 70 μmol L<sup>-1</sup>. A potential TOU of 7 mmol m<sup>-2</sup> d<sup>-1</sup> was  
26 measured and a potential DOU of 5.6 ±0.5 was modeled from the volumetric rates and DBL  
27 thickness obtained by the microsensor profiles. The contribution of DOU was lowest in the  
28 oxic zone (30%), and increased with decreasing TOU towards the oxic-hypoxic (60%) and  
29 hypoxic-anoxic zone (80%) (Table 2).

### 1 3.4 Sediment geochemistry

2 Cores from all sites had the typical vertical zonation of modern Black Sea sediments with a  
3 brown/black fluffy layer (oxic and hypoxic zones, Fig. S2d), or dark/grey fluffy layer (anoxic-  
4 sulfidic zone), covering beige-grey, homogenous, fine-grained mud. Substantial differences in  
5 the concentration profiles and volumetric production and consumption rates of dissolved iron,  
6 dissolved manganese, sulfide, and ammonium were found in pore waters from surface  
7 sediments sampled from the four different oxygen regimes (Fig. 7). In the oxic zone,  
8 dissolved iron and manganese were present in the pore water with maximal concentrations of  
9  $217 \mu\text{mol L}^{-1}$  (Fig. 7a) and  $30 \mu\text{mol L}^{-1}$  (Fig. 7b), respectively, and no free sulfide was  
10 detected (Fig. 7c). In the oxic-hypoxic zone, concentrations of dissolved iron were reduced  
11 (max.  $89 \mu\text{mol L}^{-1}$ , Fig. 7h), manganese concentrations were below detection (Fig. 7i), but  
12 free sulfide was still not present in the pore waters (Fig. 7j). In the hypoxic-anoxic zone  
13 dissolved iron and sulfide concentrations were below or close to detection limit (Fig. 7o, q),  
14 and some dissolved manganese was present in the lower part of the sediment (Fig. 7p). The  
15 station in the anoxic-sulfidic zone had no dissolved iron and manganese, but pore water  
16 concentrations of sulfide increased to up to  $1000 \mu\text{mol L}^{-1}$  at 30 cm sediment depth (Fig. 7v-x).  
17 Nitrate concentrations were  $1 \mu\text{mol L}^{-1}$  in the first centimeter of the sediment in the oxic and  
18 the oxic-hypoxic zone and dropped below detection limit in the deeper sections. Nitrate was  
19 not detected in the sediments of the hypoxic-anoxic or the anoxic-sulfidic zone (data not  
20 shown). Ammonium concentrations increased with increasing sediment depth in the top few  
21 cm of sediments sampled from the oxic to hypoxic zone ( $0\text{-}100 \mu\text{mol L}^{-1}$ ) and the anoxic-  
22 sulfidic zone ( $0\text{-}300 \mu\text{mol L}^{-1}$ ), but rates of ammonium production upon organic carbon  
23 degradation were generally low ( $< 0.6 \text{ mmol m}^{-3} \text{ d}^{-1}$ , Fig. 7d, k, r, y).

24 In solid phase extractions, reactive iron was elevated in the 0-1 cm interval of the oxic zone  
25 and iron oxides were present throughout the upper 30 cm of surface sediments (Fig. 7e). In  
26 contrast, concentrations of iron-oxides in the upper 10 cm of the oxic-hypoxic zone were  
27 clearly reduced and dropped to background concentrations below 10 cm. The same trend was  
28 observed in sediments of the hypoxic-anoxic and the anoxic-sulfidic zone (Fig. 7l, s, z). Solid  
29 phase manganese concentration was only clearly elevated in the 0-1 cm interval of the oxic  
30 zone (Fig. 7f) and at or close to background concentration below 1 cm, as in all other zones  
31 (Fig. 7m, t, aa).

1 Although pore water concentrations of sulfide were below detection limit in the oxic to  
2 hypoxic-anoxic zones, the presence of reduced solid sulfide phases (AVS, CRS and  $S^0$ , Fig. 7g,  
3 n, u, ab) and measured sulfate reduction rates indicate that some sulfate reduction took place  
4 below the oxygenated sediment. Sulfate reduction rates, integrated over the upper 10 cm of  
5 the sediment, represent gross sulfide production and compare well to net sulfide fluxes  
6 calculated from the pore water profiles in Table 3. Altogether, seafloor sulfate reduction rates  
7 were increasing nearly 40-fold from  $<0.1 \text{ mmol m}^{-2} \text{ d}^{-1}$  in the oxic zone to  $3.7 \text{ mmol m}^{-2} \text{ d}^{-1}$  in  
8 the anoxic-sulfidic zone. In all cores sulfate concentrations were constant with  $16 \text{ mmol L}^{-1}$   
9 over the upper 30 cm of the sediment (data not shown). Organic carbon content in the first cm  
10 of the sediment was lowest in the oxic zone ( $2.7 \pm 1.0 \%$  dw), nearly doubled in the oxic-  
11 hypoxic zone ( $4.6 \pm 0.9 \%$  dw) and highest in the hypoxic-anoxic zone ( $5.8 \pm 1.7 \%$  dw), Table  
12 2.

### 13 **3.5 Sediment accumulation and bioturbation**

14 Sediment porosity was similar across all sites with  $0.9 \pm 0.03$  in the top cm and  $0.8 \pm 0.07$   
15 averaged over the top 10 cm. Sediment accumulation rates, calculated from the decrease of  
16  $^{210}\text{Pb}_{\text{xs}}$  with depth and cumulative dry weight, varied around  $1 \pm 0.5 \text{ mm yr}^{-1}$  for the upper 10  
17 cm of the oxic-hypoxic and the hypoxic-sulfidic zone (Fig. S4). Nearly constant  $\ln^{210}\text{Pb}_{\text{xs}}$   
18 values in the upper 2 cm of the oxic zone indicate active sediment mixing by bioturbation. In  
19 all other zones, the linear decrease starting right below the sediment surface indicates a  
20 continuous decay and, hence, the absence of sediment mixing processes. A stronger  
21 bioturbation at the oxic site as compared to the oxic-hypoxic and hypoxic-anoxic site matches  
22 the micro-topographies observed at the different sites. Average absolute roughness heights at  
23 a water depth of 104 m were generally  $\sim 1.8$ ,  $\sim 3.2$ , and  $\sim 3.9$  times larger than at 138, 155, and  
24 206 m depth, respectively, at all investigated length scales (i.e., averaging windows). At an  
25 averaging window of 50 mm, a horizontal scale that covers many biogenic roughness  
26 elements, e.g., fecal mounds or funnels of burrows, average absolute deviations from the  
27 smoothed surface were  $0.42 \pm 0.16 \text{ mm}$  at 104 m,  $0.23 \pm 0.03 \text{ mm}$  at 138 m,  $0.15 \pm 0.03 \text{ mm}$  at  
28 155 m, and  $0.13 \pm 0.01 \text{ mm}$  at 206 m water depth. Figure S3 shows example 3D micro-  
29 topographies and extracted profiles (original and smoothed at 155 mm window size).

30

## 1 4 Discussion

### 2 4.1 Effect of oxygen availability on remineralization rates and reoxidation 3 processes

4 Rates of benthic oxygen consumption are governed by a variety of factors including primary  
5 production, particle export, quality of organic matter, bottom water oxygen concentrations,  
6 and faunal biomass (Jahnke et al., 1990; Middelburg and Levin, 2009; Wenzhöfer and Glud,  
7 2002). Here we investigated the effects of variable hypoxic conditions, with bottom water  
8 oxygen concentrations ranging from 180-0  $\mu\text{mol L}^{-1}$  within one region of similar productivity  
9 and particle flux. On the outer Western Crimean Shelf rapid and frequent variations of oxygen  
10 concentrations included strong drops in oxygen concentrations within hours, lasting for up to  
11 a few days (Fig. S1b). Such events are likely connected to the special hydrological system of  
12 the area, including the strongly variable Sevastopol Eddy (Murray and Yakushev, 2006), that  
13 is known to be of importance for the ventilation of the Crimean Shelf (Stanev et al., 2002),  
14 possibly in combination with internal waves (Luth et al., 1998; Staneva et al., 2001).

15 Oxygen consumption in the sediment is usually directly proportional to the total carbon  
16 oxidation rate, i.e. carbon oxidized by both aerobic and anaerobic pathways. An imbalance  
17 could be the result of denitrification processes, where the reduced product is  $\text{N}_2$  gas which is  
18 not further involved in sedimentary redox processes, and therefore has no direct bearing on  
19 the oxygen budget (Canfield et al., 1993a). Porewater nitrate concentrations below or close to  
20 the detection limit ( $<1 \mu\text{mol L}^{-1}$ ), suggest that at the time and place of the investigation  
21 denitrification might not have been a dominant process in organic carbon degradation.  
22 Similarly, the sulfide produced by sulfate reduction could precipitate with dissolved iron  
23 without directly consuming oxygen. However solid phase concentrations of iron-solid  
24 minerals were generally low, which indicates that sulfide precipitation most likely is not an  
25 important pathway for sulfide removal in these sediments. Assuming an annual surface  
26 primary productivity of  $220 \text{ g C m}^{-2} \text{ yr}^{-1}$ , and a particulate organic carbon (POC) export flux  
27 of around 30 % (Grégoire and Friedrich, 2004), about  $15 \text{ mmol C m}^{-2} \text{ d}^{-1}$  is expected to reach  
28 the seafloor in the investigated area. Based on ocean color satellite data from the studied area,  
29 changes in productivity and organic matter flux along the transect are negligible (10 years  
30 time frame *MyOcean* data set; [http://marine.copernicus.eu/web/69-myocan-interactive-catalogue.php?option=com\\_csw&view=details&product\\_id=OCEANCOLOUR\\_BS\\_CHL\\_L](http://marine.copernicus.eu/web/69-myocan-interactive-catalogue.php?option=com_csw&view=details&product_id=OCEANCOLOUR_BS_CHL_L)  
31 [3 REP OBSERVATIONS 009 071](#); data not shown). With a respiratory quotient of 1 (i.e.,  
32



1 one mole of oxygen consumed per one mole of CO<sub>2</sub> produced, Canfield et al., 1993a), the  
2 average TOU observed in the oxic zone would be sufficient to remineralize nearly all of the  
3 organic carbon input to the seafloor (Table 2), with oxygen fluxes measured in this study  
4 being similar to those previously reported from the same area (Table 4, including references;  
5 Grégoire and Friedrich, 2004). This suggests that within the oxic zone, most deposited carbon  
6 is directly remineralized and little carbon is escaping benthic consumption. However, already  
7 in the oxic-hypoxic zone, total benthic respiration decreased by 50 %. In the hypoxic-anoxic  
8 zone it further decreased to 10%, along with decreases in the abundance and composition of  
9 some macrofauna detected in the sediments (Table S1). Accordingly, more organic carbon got  
10 preserved in the sediment (Table 2). Through bioturbation and aeration of sediments,  
11 macrofauna can enhance total as well as microbially-driven remineralization rates. Hence,  
12 absence of macrofauna and low bioturbation activity in areas with temporary hypoxia will  
13 affect biogeochemical processes (Levin et al., 2009, and discussion below). In our study area,  
14 macrofauna abundance estimates, visual observations, as well as radiotracer and roughness  
15 assessments show that already under oxic-hypoxic conditions, sediment aeration by fauna  
16 drops rapidly. Consequently, at the onset of hypoxia, substantial amounts of organic matter  
17 accumulate in the sediments. Another effect of variable hypoxic conditions on organic matter  
18 remineralization rates is the reduced exposure time to oxygen during organic matter  
19 degradation (oxygen exposure time: oxygen penetration depth/sediment accumulation). At a  
20 sediment deposition rate of 1 mm yr<sup>-1</sup>, as estimated from <sup>210</sup>Pb measurements, particles  
21 deposited at the oxic site, are exposed much longer to aerobic mineralization processes (> 5  
22 yr) compared to the other zones (0.4 - 1.6 yr). Earlier studies showed that oxygen availability  
23 can be a key factor in the degradability of organic carbon and some compounds such as  
24 chlorophyll (King 1995) and amino acids (Vandewiele et al., 2009) will favorably accumulate  
25 in the sediments exposed to hypoxic conditions.

26 To evaluate the contribution of chemical reoxidation to TOU at the outer Western Crimean  
27 Shelf, we fitted measured pore water profiles of dissolved manganese, iron, ammonium, and  
28 sulfide with 1-D models to quantify upward directed fluxes (Berg et al., 1998, Table 3, Fig. 7).  
29 Taking the stoichiometries of the reaction of oxygen with the reduced species into account,  
30 the maximal oxygen demand for the reoxidation of reduced pore water species was less than  
31 8% (Table 3). This is less than in other studies in eutrophic shelf sediments, where the  
32 chemical and microbial reoxidation of reduced compounds, such as sulfide, dominated and

1 the heterotrophic respiration by fauna contributed around 25 % to total oxygen consumption  
2 (Glud, 2008; Heip et al., 1995; Jørgensen, 1982; Konovalov et al., 2007; Soetaert et al., 1996).

#### 3 **4.2 Effect of bottom water fluctuations on faunal respiration and diffusive** 4 **oxygen uptake**

5 Comparing total remineralization rates across all zones, including the oxygen demand by  
6 anaerobic microbial processes (Table 3), the capacity of the benthic communities to  
7 remineralize the incoming particle flux decreased from the oxic zone, to the oxic-hypoxic,  
8 hypoxic-anoxic and the anoxic zone. Total remineralization rates were similar in the hypoxic-  
9 anoxic and stable anoxic zone, but only in the latter, anaerobic processes dominated, most  
10 likely due to the persistent absence of oxygen, allowing anaerobic microbial communities to  
11 thrive.

12 Total oxygen uptake (TOU), as measured in situ with benthic chambers, represents an  
13 integrated measure of diffusive microbial respiration, as well as oxygen uptake by benthic  
14 fauna. The diffusive oxygen uptake (DOU), as calculated from microsensor profiles,  
15 represents mainly aerobic respiration of microorganisms or - although not relevant in our area  
16 (see above) - chemical reoxidation (Glud (2008)). In general, the DOU of the outer Western  
17 Crimean Shelf sediments was lower than in other shelf zones with seasonally hypoxic water  
18 columns (e.g., Glud et al. 2003), but in the same range as fluxes reported in other Black Sea  
19 studies (Table 4). Average DOU was similar in the oxic and oxic-hypoxic zone and only  
20 clearly reduced when oxygen concentrations were close to zero ( $20 \mu\text{mol L}^{-1}$ ). To test if lower  
21 fluxes at reduced bottom water oxygen concentrations rather reflect lowered efficiency of  
22 oxygen consumption processes (i.e., rate limitation), or decreased diffusional uptake (i.e.,  
23 transport limitation), we calculated the highest possible oxygen fluxes theoretically supported  
24 by the measured bottom water oxygen concentration. For this we assumed complete  
25 consumption of oxygen at the sediment surface (i.e., oxygen penetration depth approaches  
26 zero and volumetric rates approaches infinity), and calculated the flux from measured  $\text{O}_2$   
27 concentrations in the bottom water and the observed diffusive boundary layer thickness of 500  
28  $\mu\text{m}$  using Ficks' first law of diffusion (Eq. 1). Maximum theoretical fluxes were 4.3 to 36.4  
29  $\text{mmol m}^{-2} \text{d}^{-1}$  for the oxic-hypoxic zone and 2.7 to 4.6  $\text{mmol m}^{-2} \text{d}^{-1}$  for the hypoxic-anoxic  
30 zone (for oxygen concentrations see Table 4). Thus, while fluxes are generally not transport  
31 limited, the benthic uptake of oxygen approaches its potential maximum when bottom water  
32 oxygenation decreases.

1 Despite a relatively uniform sediment accumulation rate, TOU at the oxic-hypoxic zone was  
2 substantially lower as compared to the oxic zone despite bottom water oxygen concentrations  
3 remained mostly above the common threshold for hypoxia of  $63 \mu\text{mol L}^{-1}$  (Fig. 2, 5). This  
4 indicates that total oxygen uptake is more sensitive to varying bottom water oxygen  
5 concentrations than diffusive uptake mediated by microorganisms. To quantify the extent to  
6 which benthos-mediated oxygen uptake (BMU) is affected by dynamic oxygen conditions,  
7 BMU was calculated from the difference between TOU and DOU (Glud, 2008; Wenzhöfer  
8 and Glud, 2004). BMU includes not only oxygen demand of the fauna itself but also oxygen  
9 consumption that is related to the increase in oxygen-exposed sediment area due to sediment  
10 ventilation and reworking by faunal activity. Based on these calculations we assume that up to  
11 70 % of the total oxygen uptake in the oxic zone, 40 % in the oxic-hypoxic zone and 20% in  
12 the hypoxic-anoxic zone is due to benthos-mediated oxygen uptake. The remaining share (30,  
13 60, 80 %, respectively) will mainly be channeled directly into the aerobic degradation of  
14 organic carbon by microbes (and potentially also some meiofauna). A BMU of 70 % ( $10.3$   
15  $\text{mmol m}^{-2} \text{d}^{-1}$ ) in the oxic zone was considerably higher than values of 15-60 % reported from  
16 shelf sediments underlying both normoxic (Glud et al., 1998; Heip et al., 2001; Moodley et al.,  
17 1998; Piepenburg et al., 1995) and hypoxic water columns (Archer and Devol, 1992;  
18 Wenzhöfer et al., 2002). A BMU of 40 % in the oxic-hypoxic zone was still well within the  
19 ranges of some normoxic water columns (Glud et al., 1998; Heip et al., 2001; Moodley et al.,  
20 1998; Piepenburg et al., 1995).

21 It has previously been shown that sediment-water exchange rates can be altered due to  
22 changes in fauna composition in response to different bottom water oxygenation (Dale et al.,  
23 2013; Rossi et al., 2008). Coastal hypoxic zones often show reduced faunal abundances,  
24 biodiversity, and loss of habitat diversity below a threshold of  $63 \mu\text{mol O}_2 \text{L}^{-1}$  (Diaz, 2001;  
25 Levin et al., 2009). In dynamic coastal hypoxic zones with fluctuating conditions as the  
26 Kattegat (Diaz, 2001), off the coast of New York/New Jersey (Boesch and Rabalais, 1991), or  
27 the Romanian Shelf of the Black Sea (Friedrich et al., 2014), mass mortality has been reported  
28 when oxygen concentrations drop below  $22 \mu\text{mol L}^{-1}$  ( $0.5 \text{ml L}^{-1}$ ) (Levin, 2003; Levin et al.,  
29 2009). In contrast, in regions under stable low-oxygen conditions faunal communities can be  
30 adapted to such physiologically challenging conditions, for example in long-term oxygen  
31 minimum zones in the SE-Pacific, tropical E-Atlantic and N-Indian Ocean (Levin et al., 2009).  
32 In some of these areas, higher faunal biomasses have been observed at the lower boundary of  
33 the OMZ, partially explained by higher food availability (Mosch et al., 2012). Furthermore,

1 the thresholds for faunal activity can reach much lower oxygen concentrations than in regions,  
2 which are facing periodic hypoxia (Levin et al., 2009, Levin 2003). Also in the outer Western  
3 Crimean Shelf area, the overall reduction of BMU from the oxic zone to the oxic-hypoxic  
4 zone relates well with changes in some macrobenthos composition. In the oxic zone the  
5 higher fauna-mediated uptake was probably partly caused by irrigation and bioturbation by  
6 polychaetes, bivalves, and gastropods (Table S1). Ventilation of the upper sediment layer is  
7 indicated by the presence of oxidized Fe and Mn solid phase minerals in the oxic zone and in  
8 the upper 10 cm of the oxic-hypoxic zone (Fig. 7). Decreased bioturbation in the other zones  
9 is due to reduced abundances of sediment infauna. Loss of sediment ventilation also explains  
10 changes in sediment biogeochemistry, in particular the ceasing of the iron and manganese  
11 cycle upon lower bottom water oxygen concentrations (Fig. 7). In contrast, oxidized forms of  
12 iron and manganese are abundant in the surface sediments of the oxic zone. This is in  
13 accordance with previous studies that have shown that reoxidation of reduced iron and  
14 manganese is mainly stimulated by bioturbation, and thus recycling efficiency of the metals  
15 primarily depends on bottom-water oxygen levels and rates of bioturbation (Canfield et al.,  
16 1993b; Thamdrup et al., 2000; Wijsman et al., 2001).

17 The restriction of bivalves and gastropods to the upper oxic-hypoxic zone is surprising, as  
18 representatives of these groups are known to be able to maintain their respiration rate at  
19 hypoxic oxygen concentrations (Bayne, 1971; Taylor and Brand, 1975). Oxygen  
20 concentrations on the outer Western Crimean Shelf (Fig. 2) were mostly well above reported  
21 oxygen thresholds, e.g.,  $50 \mu\text{mol L}^{-1}$  for bivalves and  $25 \mu\text{mol L}^{-1}$  for gastropods (Keeling et  
22 al., 2010; Vaquer-Sunyer and Duarte, 2008). While mollusc distribution indicated low  
23 hypoxia-tolerance for the species found in the area, fish were observed in the hypoxic-anoxic  
24 zone at oxygen concentrations as low as  $<20 \mu\text{mol L}^{-1}$ , which although beyond previously-  
25 reported tolerance thresholds (Gray et al., 2002; Pihl et al., 1991; Vaquer-Sunyer and Duarte,  
26 2008), is consistent with the adaptations of some fish species of the Black Sea (Silkin and  
27 Silkina, 2005).

28 The overall role of meiobenthos in oxygen consumption is difficult to assess as it can add to  
29 both BMU and DOU by bio-irrigating the sediment as well as enhancing diffusional fluxes  
30 (Aller and Aller, 1992; Berg et al., 2001; Rysgaard et al., 2000; Wenzhöfer et al., 2002).  
31 Altogether, different distribution patterns were found for meiofauna as compared to  
32 macrofauna. Meiobenthos abundances were similar in the oxic and oxic-hypoxic zone, and  
33 only sharply decreased in the hypoxic-anoxic zone. As shown previously (Levin et al., 2009)

1 nematodes and foraminifera dominate meiofauna in hypoxic zones due to their ability to adapt  
2 to low oxygen concentrations. In particular, nematodes are known to tolerate hypoxic,  
3 suboxic, anoxic or even sulfidic conditions (Sergeeva et al., 2012; Sergeeva and Zaika, 2013;  
4 Steyaert et al., 2007; Van Gaever et al., 2006). Some meiobenthos species are known to occur  
5 under hypoxic conditions (Sergeeva and Anikeeva, 2014; Sergeeva et al., 2013). The  
6 relatively high abundance of apparently living foraminifera in the hypoxic zone might be  
7 related to the ability of some species to respire nitrate under anoxic conditions (Risgaard-  
8 Petersen et al., 2006).

9 Regarding the validation of the traditionally-used hypoxia threshold for impact on fauna (63  
10  $\mu\text{mol O}_2 \text{ L}^{-1}$ , e.g., Diaz, 2001), our results support previous studies where significant changes  
11 in community structure were reported already at the onset of hypoxia (Gray et al., 2002;  
12 Steckbauer et al., 2011; Vaquer-Sunyer and Duarte, 2008). Our results indicate that fauna-  
13 mediated oxygen uptake and biogeochemical fluxes are strongly reduced already at periodical  
14 hypoxic conditions, as caused by transport of low-oxygen waters via internal waves or eddies  
15 close to the shelf break.

## 16 **5. Conclusions**

17 This study assesses the effect of different ranges of bottom water oxygenation and its local  
18 fluctuations on carbon remineralization rates, the proportion of microbial vs. fauna-mediated  
19 respiration, benthic community structure and the share of anaerobic vs. aerobic microbial  
20 respiration pathways. We could show that fauna-mediated oxygen uptake and biogeochemical  
21 fluxes can be strongly reduced already at periodically hypoxic conditions around  $63 \mu\text{mol L}^{-1}$ .  
22 The diffusive respiration by microbes and small metazoa decreased substantially only when  
23 oxygen concentration dropped below  $20 \mu\text{mol L}^{-1}$ . The oxidation of upward diffusing reduced  
24 compounds from pore water only played a minor role in the diffusive uptake of oxygen by the  
25 sediment, in contrast to previous studies of shelf and upper margin sediments. Hypoxia leads  
26 to a substantial decrease of the efficiency of carbon degradation compared to persistently  
27 oxygenated zones, where nearly all of the deposited carbon is rapidly mineralized by aerobic  
28 respiration. Consequently, already at the onset of hypoxia, or under fluctuating conditions  
29 such as caused by internal waves or eddies, substantial amounts of organic matter can  
30 accumulate in marine sediments, and ecosystem functioning could be impacted over much  
31 larger areas adjacent to hypoxic ecosystems.

1

## 2 **Acknowledgements**

3 We thank the Captain and shipboard crew of the RV Maria S. Merian, the JAGO team  
4 (GEOMAR, Kiel) and shipboard scientists of the cruise MSM 15/1 for their excellent work at  
5 sea. We are grateful for technical assistance from Rafael Stiens, Martina Alisch, Erika Weiz,  
6 and Kirsten Neumann. We thank the Sea-Tech technicians of the HGF MPG Joint Research  
7 Group for Deep-Sea Ecology and Technology (MPI-AWI) for the construction and  
8 maintenance of the in situ devices and the technicians of the Microsensor Group for the  
9 construction of microsensors. We thank Tim Ferdelman and Gail Lee Arnold for help with the  
10 sedimentation rate measurements. This project was financed by the EU 7th FP project  
11 HYPOX (*In situ monitoring of oxygen depletion in hypoxic ecosystems of coastal and open*  
12 *seas, and land-locked water bodies*) EC Grant 226213.

13

## 1 References

- 2
- 3 Abril, G., Commarieu, M.-V., Etcheber, H., Deborde, J., Deflandre, B., Živadinović, M. K.,  
4 Chaillou, G., and Anschutz, P.: In vitro simulation of oxic/suboxic diagenesis in an  
5 estuarine fluid mud subjected to redox oscillations, *Estuarine, Coastal and Shelf*  
6 *Science*, 88, 279-291, 2010.
- 7 Aller, R. and Aller, J.: Meiofauna and solute transport in marine muds, *Limnology and*  
8 *Oceanography* 37, 1018-1033, 1992.
- 9 Archer, D. and Devol, A.: Benthic oxygen fluxes on the Washington shelf and slope: A  
10 comparison of in situ microelectrode and chamber flux measurements, *Limnology and*  
11 *Oceanography*, 37, 614-629, 1992.
- 12 Baird, D., Christian, R. R., Peterson, C. H., and Johnson, G. A.: Consequences of hypoxia on  
13 estuarine ecosystem function: energy diversion from consumers to microbes,  
14 *Ecological Applications*, 14, 805-822, 2004.
- 15 Bayne, B. L.: Oxygen consumption by three species of lamellibranch mollusc in declining  
16 ambient oxygen tension, *Comparative Biochemistry and Physiology Part A:*  
17 *Physiology*, 40, 955-970, 1971.
- 18 Berg, P., Risgaard-Petersen, N., and Rysgaard, S.: Interpretation of measured concentration  
19 profiles in sediment pore water, *Limnology and Oceanography*, 43, 1500-1510, 1998.
- 20 Berg, P., Rysgaard, S., Funch, P., and Sejr, M.: Effects of bioturbation on solutes and solids in  
21 marine sediments, *Aquatic Microbial Ecology* 26, 81-94, 2001.
- 22 Boesch, D. F. and Rabalais, N. N.: Effects of hypoxia on continental shelf benthos:  
23 comparisons between the New York Bight and the Northern Gulf of Mexico, in:  
24 *Modern and Ancient Continental Shelf Anoxia*, edited by: Tyson, R. V. and Pearson, T.  
25 H., Geological Society Special Publication 58, 27-34, Geological Soc., London, 1991.
- 26 Boetius, A. and Wenzhöfer, F.: In situ technologies for studying deep-sea hotspot ecosystems,  
27 *Oceanography*, 22, p 177, doi: 10.5670/oceanog.2009.17, 2009.
- 28 Broecker, W. S. and Peng, T. H.: Gas exchange rates between air and sea, *Tellus*, 26, 21-35,  
29 1974.

- 1 Canfield, D. E., Jørgensen, B. B., Fossing, H., Glud, R., Gundersen, J., Ramsing, N. B.,  
2 Thamdrup, B., Hansen, J. W., Nielsen, L. P., and Hall, P. O. J.: Pathways of organic  
3 carbon oxidation in three continental margin sediments, *Marine Geology*, 113, 27-40,  
4 1993a.
- 5 Canfield, D. E., Thamdrup, B., and Hansen, J. W.: The anaerobic degradation of organic  
6 matter in Danish coastal sediments: Iron reduction, manganese reduction, and sulfate  
7 reduction, *Geochim Cosmochim Acta*, 57, 3867-3883, 1993b.
- 8 Clarke, K.-R.: Non - parametric multivariate analyses of changes in community structure,  
9 *Australian Journal of Ecology*, 18, 117-143, 1993.
- 10 Cline, J. D.: Spectrophotometric determination of hydrogen sulfide in natural waters,  
11 *Limnology and Oceanography*, 14, 454-458, 1969.
- 12 Cook, P. L. M., Wenzhöfer, F., Glud, R. N., Janssen, F., and Huettel, M.: Benthic solute  
13 exchange and carbon mineralization in two shallow subtidal sandy sediments: Effect  
14 of advective pore-water exchange, *Limnology and Oceanography* 1943-1963, 2007.
- 15 Dale, A. W., Bertics, V. J., Treude, T., Sommer, S., and Wallmann, K.: Modeling benthic–  
16 pelagic nutrient exchange processes and porewater distributions in a seasonally  
17 hypoxic sediment: evidence for massive phosphate release by *Beggiatoa*?,  
18 *Biogeosciences*, 10, 629-651, 2013.
- 19 de Beer, D., Glud, A., Epping, E., and Kuhl, M.: A fast-responding CO<sub>2</sub> microelectrode for  
20 profiling sediments, microbial mats, and biofilms, *Limnology and Oceanography*, 42,  
21 1590-1600, 1997.
- 22 Diaz, R. J.: Overview of hypoxia around the world, *Journal of Environmental Quality*, 30,  
23 275-281, 2001.
- 24 Fossing, H. and Jørgensen, B. B.: Measurement of bacterial sulfate reduction in sediments:  
25 evaluation of a single-step chromium reduction method, *Biogeochemistry*, 8, 205-222,  
26 1989.
- 27 Friedl, G., Dinkel, C., and Wehrli, B.: Benthic fluxes of nutrients in the northwestern Black  
28 Sea, *Marine Chemistry*, 62, 77-88, 1998.
- 29 Friedrich, J., Janssen, F., Aleynik, D., Bange, H. W., Boltacheva, N., Çagatay, M. N., Dale, A.  
30 W., Etiope, G., Erdem, Z., Geraga, M., Gilli, A., Gomoiu, M. T., Hall, P. O. J.,



- 1       Hansson, D., He, Y., Holtappels, M., Kirf, M. K., Kononets, M., Konovalov, S.,  
2       Lichtschlag, A., Livingstone, D. M., Marinaro, G., Mazlumyan, S., Naeher, S., North,  
3       R. P., Papatheodorou, G., Pfannkuche, O., Prien, R., Rehder, G., Schubert, C. J.,  
4       Soltwedel, T., Sommer, S., Stahl, H., Stanev, E. V., Teaca, A., Tengberg, A.,  
5       Waldmann, C., Wehrli, B., and Wenzhöfer, F.: Investigating hypoxia in aquatic  
6       environments: diverse approaches to addressing a complex phenomenon,  
7       *Biogeosciences*, 11, 1215-1259, 2014.
- 8       Glud, R. N.: Oxygen dynamics of marine sediments, *Marine Biology Research*, 4, 243–289,  
9       2008.
- 10      Glud, R. N., Gundersen, J. K., Røy, H., and Jørgensen, B. B.: Seasonal dynamics of benthic  
11      O<sub>2</sub> uptake in a semi-enclosed bay: Importance of diffusion and faunal activity,  
12      *Limnology and Oceanography*, 48, 1265-1276, 2003.
- 13      Glud, R. N., Holby, O., Hoffmann, F., and Canfield, D. E.: Benthic mineralization and  
14      exchange in Arctic sediments (Svalbard, Norway), *Marine Ecology Progress Series*,  
15      173, 237-251, 1998.
- 16      Grasshoff, K.: *Methods of seawater analysis*, Verlag Chemie, Weinheim, 1983.
- 17      Gray, J. S., Wu, R. S.-s., and Or, Y. Y.: Effects of hypoxia and organic enrichment on the  
18      coastal marine environment, *Marine Ecology Progress Series*, 238, 249–279, 2002.
- 19      Grego, M., Stachowitsch, M., De Troch, M., and Riedel, B.: CellTracker Green labelling vs.  
20      rose bengal staining: CTG wins by points in distinguishing living from dead anoxia-  
21      impacted copepods and nematodes, *Biogeosciences*, 10, 4565-4575, 2013.
- 22      Grégoire, M. and Friedrich, J.: Nitrogen budget of the north-western Black Sea shelf as  
23      inferred from modeling studies and in-situ benthic measurements, *Marine Ecology*  
24      *Progress Series*, 270, 15-39, 2004.
- 25      Heip, C. H. R., Duineveld, G., Flach, E., Graf, G., Helder, W., Herman, P. M. J., Lavaleye, M.,  
26      Middelburg, J. J., Pfannkuche, O., Soetaert, K., Soltwedel, T., de Stigter, H., Thomsen,  
27      L., Vanaverbeke, J., and de Wilde, P.: The role of the benthic biota in sedimentary  
28      metabolism and sediment-water exchange processes in the Goban Spur area (NE  
29      Atlantic), *Deep Sea Research Part II: Topical Studies in Oceanography*, 48, 3223-3243,  
30      2001.

- 1 Heip, C. H. R., Goosen, N. K., Herman, P. M. J., Kromkamp, J., Middelburg, J. J., and  
2 Soetaer, K.: Production and consumption of biological particles in temperate tidal  
3 estuaries, *Ann. Rev. Ocean. Mar. Biol.*, 33, 1–150, 1995.
- 4 Holtappels, M., Glud, R. N., Donis, D., Liu, B., Hume, A., Wenzhöfer, F., and Kuypers, M.  
5 M. M.: Effects of transient bottom water currents and oxygen concentrations on  
6 benthic exchange rates as assessed by eddy correlation measurements, *Journal of*  
7 *Geophysical Research: Oceans*, 118, 1157-1169, 2013.
- 8 Holtappels, M., Kuypers, M. M., Schlüter, M., and Brüchert, V.: Measurement and  
9 interpretation of solute concentration gradients in the benthic boundary layer,  
10 *Limnology and Oceanography: Methods*, 9, 1-13, 2011.
- 11 Jahnke, R. A., Reimers, C. E., and Craven, D. B.: Intensification of recycling of organic  
12 matter at the sea floor near ocean margins, *Nature*, 348, 50-54, 1990.
- 13 Jeroschewski, P., Steuckart, C., and Kühl, M.: An amperometric microsensor for the  
14 determination of H<sub>2</sub>S in aquatic environments, *Analytical Chemistry*, 68, 4351-4357,  
15 1996.
- 16 Jørgensen, B. B.: A comparison of methods for the quantification of bacterial sulfate  
17 reduction in coastal marine sediments, *Geomicrobiology Journal*, 1, 11-27, 1978.
- 18 Jørgensen, B. B.: Mineralization of organic matter in the sea bed—the role of sulphate  
19 reduction, *Nature*, 643-645, 1982.
- 20 Kallmeyer, J., Ferdelman, T. G., Weber, A., Fossing, H., and Jørgensen, B. B.: A cold  
21 chromium distillation procedure for radiolabeled sulfide applied to sulfate reduction  
22 measurements, *Limnology and Oceanography: Methods*, 2, 171-180, 2004.
- 23 Keeling, R. F., Kortzinger, A., and Gruber, N.: Ocean deoxygenation in a warming world,  
24 *Annual Review of Marine Science* 2, 199-229 2010.
- 25 King, L. L.: A mass balance of chlorophyll degradation product accumulation in Black Sea  
26 sediments, *Deep Sea Research Part I: Oceanographic Research Papers* 42, 919-942,  
27 1995.
- 28 Konovalov, S. K., Luther III, G. W., and Yücel, M.: Porewater redox species and processes in  
29 the Black Sea sediments, *Chemical Geology*, 245, 254-274, 2007.

- 1 Levin, L. A.: Oxygen minimum zone benthos: adaptation and community response to hypoxia,  
2 Oceanogr. Mar. Biol. Ann. Rev., 41, 1–45, 2003.
- 3 Levin, L. A., Ekau, W., Gooday, A. J., Jorissen, F., Middelburg, J. J., Naqvi, W., Neira, C.,  
4 Rabalais, N. N., and Zhang, J.: Effects of natural and human-induced hypoxia on  
5 coastal benthos, Biogeosciences, 6, 3563-3654, 2009.
- 6 Lichtschlag, A., Felden, J., Wenzhöfer, F., Schubotz, F., Ertefai, T. F., Boetius, A., and de  
7 Beer, D.: Methane and sulfide fluxes in permanent anoxia: In situ studies at the  
8 Dvurechenskii mud volcano (Sorokin Trough, Black Sea), Geochim Cosmochim Acta,  
9 74, 5002-5018, 2010.
- 10 Luth, U., Luth, C., Stokozov, N. A. and Gulin, M. B.: The chemocline rise effect on  
11 the northwestern slope of the Black Sea, in: Methane Gas Seep Explorations in  
12 the Black Sea (MEGASEEBS), Project Report. Ber. Zentrum Meeres- u.  
13 Klimaforsch., edited by: Luth, U., Luth, C., and Thiel, H., Univ. Hamburg,  
14 Reihe E, 14, 59–77, 1998.
- 15 Middelburg, J. J., Levin, L. A.: Coastal hypoxia and sediment biogeochemistry,  
16 Biogeosciences, 6, 1273-1293, 2009.
- 17 Moodley, L., Schaub, B. E. M., Zwaan, G. J. v. d., and Herman, P. M. J.: Tolerance of benthic  
18 foraminifera (Protista: Sarcodina) to hydrogen sulphide, Ecology Progress Series, 169,  
19 77-86, 1998.
- 20 Mosch, T., Sommer, S., Dengler, M., Noffke, A., Bohlen, L., Pfannkuche, O. Liebetraut, V.  
21 and Wallmann, K.: Factors influencing the distribution of epibenthic megafauna across  
22 the Peruvian oxygen minimum zone. Deep Sea Research Part I: Oceanographic  
23 Research Papers, 68, 123-135, 2012.
- 24 Murray, J. W. and Yakushev, E.: The suboxic transition zone in the Black Sea, in: Past and  
25 Present Marine Water Column Anoxia, edited by: Neretin, L., NATO Science Series  
26 IV: Earth and Environmental Sciences, 64, Springer, Dordrecht, 105-138,  
27 doi:10.1007/1-4020-4297-3\_05,2006.
- 28 Niggemann, J., Ferdelman, T. G., Lomstein, B. A., Kallmeyer, J., and Schubert, C. J.: How  
29 depositional conditions control input, composition, and degradation of organic matter  
30 in sediments from the Chilean coastal upwelling region, Geochim Cosmochim Acta, 71,  
31 1513-1527, 2007.

- 1 Oksanen, J., Blanchet, F. G., Kindt, R., Legendre, P., Minchin, P. R., O'Hara, R. B., Simpson,  
2 G. L., Solymos, P., Stevens, M. H. H., Wagner, H.: *vegan: Community Ecology*  
3 *Package*, R package version of The Comprehensive R Archive Network, 1.17-3, 2010.
- 4 Pearson, T. H. and Rosenberg, R.: Energy flow through the SE Kattegat: A comparative  
5 examination of the eutrophication of a coastal marine ecosystem, *Netherlands Journal*  
6 *of Sea Research*, 28, 317-334, 1992.
- 7 Piepenburg, D., Blackburn, H., T., Dorrien, v., F., C., Gutt, J., Hall, J., P. O., Hulth, S.,  
8 Kendall, A., M., Opalinski, W., K., Rachor, E., Schmid, and K., M.: Partitioning of  
9 benthic community respiration in the Arctic (northwestern Barents Sea), *Marine*  
10 *Ecology Progress Series*, 118, 199-213, 1995.
- 11 Pihl, L., Baden, S. P., and Diaz, R. J.: Effects of periodic hypoxia on distribution of demersal  
12 fish and crustaceans, *Mar. Biol.*, 108, 349-360, 1991.
- 13 Poulton, S. W. and Canfield, D. E.: Development of a sequential extraction procedure for  
14 iron: implications for iron partitioning in continentally derived particulates, *Chemical*  
15 *Geology*, 214, 209-221, 2005.
- 16 Rasmussen, H. and Jørgensen, B. B.: Microelectrode studies of seasonal oxygen uptake in a  
17 coastal sediment: role of molecular diffusion, *Marine Ecology Progress Series* 81,  
18 289-303, 1992.
- 19 Revsbech, N. P.: An oxygen microsensor with a guard cathode, *Limnol. Oceanogr.*, 34, 474-  
20 478, doi: 10.4319/lo.1989.34.2.0474, 1989.
- 21 Risgaard-Petersen, N., Langezaal, A. M., Ingvarsdén, S., Schmid, M. C., Jetten, M. S. M., Op  
22 den Camp, H. J. M., Derksen, J. W. M., Pina-Ochoa, E., Eriksson, S. P., Peter Nielsen,  
23 L., Revsbech, N. P., Cedhagen, T., and van der Zwaan, G. J.: Evidence for complete  
24 denitrification in a benthic foraminifera, *Nature*, 443, 93-96, 2006.
- 25 Rossi, F., Gribsholt, B., Middelburg, J. J., and Heip, C.: Context-dependent effects of  
26 suspension feeding on intertidal ecosystem functioning, *Marine Ecology Progress*  
27 *Series*, 354, 47-57, 2008.
- 28 Rysgaard, S., Christensen, P., Sørensen, M., Funch, P., and Berg, P.: Marine meiofauna,  
29 carbon and nitrogen mineralization in sandy and soft sediments of Disko Bay, West  
30 Greenland, *Aquatic Microbial Ecology* 21, 59-71, 2000.

- 1 Seeberg-Elverfeldt J., Schlüter M., Feseker T. and Kolling M.: Rhizon sampling of  
2 porewaters near the sediment–water interface of aquatic systems. *Limnology and*  
3 *Oceanography: Methods*, 3, 361–371, 2005.
- 4 Sergeeva, N., Gooday, A. J., Mazlumyan, S. A., Kolesnikova, E. A., Lichtschlag, A.,  
5 Koshelva, T. N., and Anikeeva, O. V.: Meiobenthos of the oxic/anoxic interface in the  
6 southwestern region of the Black Sea: abundance and taxonomic composition, in:  
7 ANOXIA: Evidence for Eukaryote Survival and Paleontological Strategies, edited by:  
8 Altenbach, A. V., Bernhard, J. M., and Seckbach, J., *Cellular Origin, Life in Extreme*  
9 *Habitats and Astrobiology*, 21, Springer, Dordrecht, 369-401, doi: 10.1007/978-94-  
10 007-1896-8\_20, 2012.
- 11 Sergeeva, N. G. and Anikeeva, O. V.: Soft-walled foraminifera under normoxia/hypoxia  
12 conditions in the shallow areas of the Black Sea, in: *Foraminifera. Aspects of*  
13 *Classification, Stratigraphy, Ecology and Evolution*, edited by: Georgescu, M. D.,  
14 Nova Publ., New York, 227-247, 2014.
- 15 Sergeeva, N. G., Mazlumyan, S. A., Çağatay, N., and Lichtschlag, A.: Hypoxic meiobenthic  
16 communities of the Istanbul Strait’s (Bosporus) outlet area of the Black Sea, *Turkish*  
17 *Journal of Fisheries and Aquatic Sciences*, 13, 33-41, 2013.
- 18 Sergeeva, N. G. and Zaika, V. E.: The Black Sea meiobenthos in permanently hypoxic habitat,  
19 *Acta zoologica bulgarica*, 65 139-150, 2013.
- 20 Silkin, Y. A. and Silkina, E. N.: Effect of hypoxia on physiological-biochemical blood  
21 parameters in some marine fish, *J Evol Biochem Phys*, 41, 527-532, 2005.
- 22 Soetaert, K., Herman, P. M. J., and Middelburg, J. J.: A model of early diagenetic processes  
23 from the shelf to abyssal depths, *Geochim Cosmochim Ac*, 60, 1019-1040, 1996.
- 24 Stanev, E. V., Beckers, J. M., Lancelot, C., Staneva, J. V., Le Traon, P. Y., Peneva, E. L., and  
25 Gregoire, M.: Coastal–open ocean exchange in the Black Sea: observations and  
26 modelling, *Estuarine, Coastal and Shelf Science*, 54, 601-620, 2002.
- 27 Stanev, E. V., He, Y., Grayek, S., and Boetius, A.: Oxygen dynamics in the Black Sea as seen  
28 by Argo profiling floats, *Geophys. Res. Lett.*, 40, 3085-3090, 2013.

- 1 Staneva, J. V., Dietrich, D. E., Stanev, E. V., and Bowman, M. J.: Rim current and coastal  
2 eddy mechanisms in an eddy-resolving Black Sea general circulation model, *Journal*  
3 *of Marine Systems*, 31, 137-157, 2001.
- 4 Steckbauer, A., Duarte, C. M., Carstensen, J., Vaquer-Sunyer, R., and Conley, D. J.:  
5 Ecosystem impacts of hypoxia: thresholds of hypoxia and pathways to recovery,  
6 *Environ. Res. Lett.*, 6, 025003 (12pp), doi: 10.1088/1748-9326/6/2/025003, 2011.
- 7 Steyaert, M., Moodley, L., Nadong, T., Moens, T., Soetaert, K., and Vincx, M.: Responses of  
8 intertidal nematodes to short-term anoxic events, *Journal of Experimental Marine*  
9 *Biology and Ecology*, 345, 175-184, 2007.
- 10 Taylor, A. C. and Brand, A. R.: A comparative study of the respiratory responses of the  
11 bivalves *Arctica islandica* (L.) and *Mytilus edulis* L. to declining oxygen tension,  
12 *Proceedings of the Royal Society of London. Series B. Biological Sciences*, 190, 443-  
13 456, 1975.
- 14 Thamdrup, B., Rosselló-Mora, R., and Amann, R.: Microbial manganese and sulfate reduction  
15 in Black Sea shelf sediments, *Applied and Environmental Microbiology* 66, 2888–  
16 2897, 2000.
- 17 Tolmazin, D.: Changing coastal oceanography of the Black Sea. I: Northwestern shelf,  
18 *Progress in Oceanography*, 15, 217-276, 1985.
- 19 Van Gaever, S., Moodley, L., de Beer, D., and Vanreusel, A.: Meiobenthos at the Arctic  
20 Håkon Mosby Mud Volcano, with a parental-caring nematode thriving in sulphide-  
21 rich sediments, *Marine Ecology Progress Series*, 321, 143-155, 2006.
- 22 Vandewiele, S., Cowie, G., Soetaert, K., and Middelburg, J. J.. Amino acid biogeochemistry  
23 and organic matter degradation state across the Pakistan margin oxygen minimum  
24 zone. *Deep Sea Research Part II: Topical Studies in Oceanography*, 56, 376-392, 2009.
- 25 Vaquer-Sunyer, R., C. M. Duarte: Thresholds of hypoxia for marine biodiversity, *Proceedings*  
26 *of the National Academy of Sciences of the United States of America*, 105, 15452–  
27 15457, 2008.
- 28 Waldmann, C. and Bergenthal, M.: CMOVE – a versatile underwater vehicle for seafloor  
29 studies, *OCEANS 2010 Proc.*, IEEE conference, 20-23 September, Seattle, WA, USA,  
30 doi:2010,10.1109/OCEANS.2010.5664261, 2010.

- 1 Weber, A., Riess, W., Wenzhoefer, F., and Jørgensen, B. B.: Sulfate reduction in Black Sea  
2 sediments: in situ and laboratory radiotracer measurements from the shelf to 2000m  
3 depth, *Deep Sea Research Part I: Oceanographic Research Papers*, 48, 2073-2096,  
4 2001.
- 5 Wenzhöfer, F. and Glud, R. N.: Benthic carbon mineralization in the Atlantic: a synthesis  
6 based on in situ data from the last decade, *Deep Sea Research Part I: Oceanographic*  
7 *Research Papers*, 49, 1255-1279, 2002.
- 8 Wenzhöfer, F. and Glud, R. N.: Small-scale spatial and temporal variability in coastal benthic  
9 O<sub>2</sub> dynamics: Effects of fauna activity, *Limnology and Oceanography*, 49, 1471-1481,  
10 2004.
- 11 Wenzhöfer, F., Riess, W., and Luth, U.: In situ macrofaunal respiration rates and their  
12 importance for benthic carbon mineralization on the northwestern Black Sea shelf,  
13 *Ophelia*, 56, 87-100, 2002.
- 14 Wijsman, J. W. M., Middelburg, J. J., and Heip, C. H. R.: Reactive iron in Black Sea  
15 sediments: Implications for iron cycling, *Mar Geol*, 172, 167-180, 2001.
- 16 Winkler, L.: The determination of dissolved oxygen in water, *Ber Dtsch Chem Ges* 21, 2843–  
17 2857, 1888.
- 18 Witte, U. and Pfannkuche, O.: High rates of benthic carbon remineralisation in the abyssal  
19 Arabian Sea, *Deep Sea Research Part II: Topical Studies in Oceanography*, 47, 2785-  
20 2804, 2000.
- 21 Zaika, V. E. and Gulin, M. B.: The maximum depths of fish inhabitation in the Black Sea and  
22 features of their trophic strategy nearly of oxic/anoxic interface, *Marine Ecology*  
23 *Journal*, 10, 39 – 47, (in Russian), 2011.
- 24 Zaika, V. E., Konovalov, S. K., and Sergeeva., N.: The events of local and seasonal hypoxia  
25 at the bottom of Sevastopol bays and their influence on macrobenthos, *Marine*  
26 *Ecology Journal*, 10, 15-25, 2011.
- 27 Zopfi, J., Ferdelman, T. G., and Fossing, H.: Distribution and fate of sulfur intermediates –  
28 sulfite tetrathionate, thiosulfate, and elemental sulfur – in marine sediments, in: *The*  
29 *Biogeochemistry of Sulfur*, GSA Special Paper, edited by: Amend, J., Edwards, K.,  
30 and Lyons, T., Geol. Soc. America, London, 97-116, 2004.

1 Table 1. Measurements and samples (including PANGAEA event labels) taken in zones with  
 2 different oxygen regime. PUC = JAGO pushcores, MOVE = benthic crawler move (in situ  
 3 microsensor measurements and /or benthic chamber deployment), TVMUC = video-guided  
 4 multicorer, KAMM = lander (in situ microsensor measurements and /or benthic chamber  
 5 deployment).

6	Zone	Water depth (m)	Station/PANGAEA event label	Position	Date	Device	Method
	<i>oxic zone</i> <130m  bottom water oxygen conc. > 63 $\mu\text{mol L}^{-1}$	101	MSM15/1_482_ PUC 1, 3, 5, 6	44° 49.00' N 33° 09.37' E	03.05.2010	PUC	Macro- and meiobenthos
		104	MSM15/1_484-1	44° 49.49' N 33° 09.32' E	03.05.2010	MOVE	Benthic oxygen uptake
		104	MSM15/1_464-1	44° 49.45' N 33° 09.26' E	02.05.2010	TVMUC	Macro- and meiobenthos
		104	MSM15/1_462-1	44° 49.45' N 33° 09.26' E	02.05.2010	TVMUC	Geochemistry
		106	MSM15/1_469-1	44° 49.46' N 33° 09.67' E	02.05.2010	KAMM	Benthic oxygen uptake
		105	MSM15/1_444_ PUC 1	44° 49.32' N 33° 09.46' E	01.05.2010	PUC	Macro- and meiobenthos
		117	MSM15/1_440_ _PUC 5, 6	44° 40.49' N 33° 05.53' E	01.05.2010	PUC	Macro- and meiobenthos
		120	MSM15/1_459-1, 2	44° 40.48' N 33° 05.53' E	02.05.2010	TVMUC	Macro- and meiobenthos
		129	MSM15/1_486_ PUC 1, 7	44° 39.13' N 33° 01.78' E	04.05.2010	PUC	Macro- and meiobenthos
	<i>oxic-hypoxic</i> (130-142 m)  bottom water oxygen conc. > 63 to > 0 $\mu\text{mol L}^{-1}$	131	MSM15/1_460_ _PUC-1	44° 39.26' N 33° 01.12' E	02.05.2010	PUC	Macro- and meiobenthos
		136	MSM15/1_487-1	44° 38.78' N 33° 00.25' E	04.05.2010	TVMUC	Geochemistry
		137	MSM15/1_434-1	44° 38.93' N 32° 59.98' E	01.05.2010	KAMM	Benthic oxygen uptake
		137	MSM15/1_455-1	44° 38.92' N 32° 59.97' E	02.05.2010	MOVE	Benthic oxygen uptake
		138	MSM15/1_489- 1, 2	44° 38.79' N 33° 00.25' E	04.05.2010	TVMUC	Macro- and meiobenthos
		140	MSM15/1_499-1	44° 38.80' N 33° 00.26' E	05.05.2010	KAMM	Benthic oxygen uptake
	<i>hypoxic-anoxic</i> (142-167 m)  bottom water oxygen conc. 63-0 $\mu\text{mol L}^{-1}$	145	MSM15/1_512-3	44° 37.39' N 32° 56.21' E	05.05.2010	PUC	Macro- and meiobenthos
		151	MSM15/1_372_ PUC 1	44° 37.46' N 32° 54. 91'E	25.04.2010	PUC	Macro- and meiobenthos
		154	MSM15/1_383-1	44° 37.74' N 32° 54.92' E	26.04.2010	KAMM	Benthic oxygen uptake
		155	MSM15/1_379-1	44° 37.55' N 32° 54.97' E	26.04.2010	TVMUC	Macro- and meiobenthos
		156	MSM15/1_386-1	44° 37.58' N 32° 54.97' E	26.04.2010	MOVE	Benthic oxygen uptake
		162	MSM15/1_374-1	44° 37.07' N 32° 53.49' E	25.04.2010	PUC	Macro- and meiobenthos
		163	MSM15/1_425-1	44° 47.09' N 31° 58.05' E	30.04.2010	TVMUC	Macro- and meiobenthos
		164	MSM15/1_393-1	44° 37.08' N 32° 53.48' E	27.04.2010	TVMUC	Geochemistry
	<i>anoxic-sulfidic zone</i> (>167m) sulfide present in anoxic bottom water	207	MSM15/1_448-1	44° 35.84' N 32° 49.03' E	01.05.2010	TVMUC	Geochemistry



1 Table 2. Diffusive oxygen uptake (DOU) rates, total oxygen uptake (TOU) rates and oxygen  
 2 penetration depth under different oxygen regimes at the outer Western Crimean Shelf.  
 3 Chamber measurements in the hypoxic-anoxic zone represent potential rates, scaled to a  
 4 bottom water oxygen concentration of 20  $\mu\text{mol O}_2 \text{ L}^{-1}$  (instead of 70  $\mu\text{mol O}_2 \text{ L}^{-1}$ ).

5

6

Zone	DOU $J_{\text{O}_2} \pm \text{SD}$ ( $\text{mmol m}^{-2}\text{d}^{-1}$ )	TOU $J_{\text{O}_2} \pm \text{SD}$ ( $\text{mmol m}^{-2}\text{d}^{-1}$ )	DOU:TOU ratio (%)	Oxygen penetration depth $\pm \text{SD}$ (mm)	$C_{\text{org}} \pm \text{SD}$ (% dw)
<i>oxic zone</i> <130m bottom water oxygen conc. > 63 $\mu\text{mol L}^{-1}$	4.6 $\pm$ 1.8 range: 2.4 to 8.1, n = 15	14.9 $\pm$ 5.1 range: 9 to 20.6, n = 5	30:70	5.3 $\pm$ 2.5	2.7 $\pm$ 1.0
<i>oxic-hypoxic</i> (130-142 m) bottom water oxygen conc. > 63 to > 0 $\mu\text{mol}$ $\text{L}^{-1}$	4.4 $\pm$ 1.9 range: 0.6 to 8.0, n = 12	7.3 $\pm$ 3.5 range: 3.2 to 9.4, n = 3	60:40	1.6 $\pm$ 1.2	4.6 $\pm$ 0.9
<i>hypoxic-anoxic</i> (142-167 m) bottom water oxygen conc. 63-0 $\mu\text{mol L}^{-1}$	1.3 $\pm$ 0.5 range: 0.8 to 2.1, n = 5 (potential rate: 5.6)	1.6 $\pm$ 0.5 <i>Modeled</i>	80:20 ( <i>modeled</i> <i>from</i> <i>potential</i> <i>rates</i> )	0.4 $\pm$ 0.1	5.8 $\pm$ 1.7

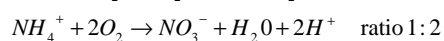
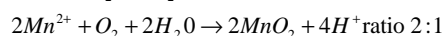
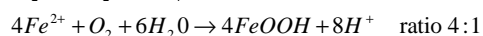
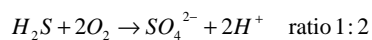
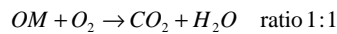
1 Table 3. Diffusive oxygen uptake compared to fluxes of reduced species, calculated from the  
 2 modeled profiles (Fig. 7) or measured directly (SRR = Sulfate reduction rates). The sum in  
 3 oxygen equivalents is calculated from the stoichiometry of the oxidation processes (respective  
 4 formulas are displayed at the lower end of the table), and oxygen available for direct aerobic  
 5 respiration is calculated by subtracting the potential oxygen demand from the available  
 6 oxygen flux.  
 7

	Oxygen flux (mmol m <sup>-2</sup> d <sup>-1</sup> )		Reduced species fluxes (mmol m <sup>-2</sup> d <sup>-1</sup> )			SUM in oxygen equivalen ts	Diffusive oxygen consumption (direct aerobic mineralization : reoxidation) in mmol m <sup>-2</sup> d <sup>-1</sup> and %
	DOU (J <sub>O2</sub> ) <i>see</i> Table 2	J <sub>Fe<sup>2+</sup></sub>	J <sub>Mn<sup>2+</sup></sub>	J <sub>sulfide / SRR</sub>	J <sub>NH<sub>4</sub><sup>+</sup></sub>		
<i>oxic zone</i> <130m, bottom water oxygen conc. > 63 μmol L <sup>-1</sup>	- 4.6	0.1	<0.1	0*/<0.1	0.1	0.23	4.38 : 0.23 95 % : 5 %
<i>oxic-hypoxic</i> 130-142 m, bottom water oxygen conc. > 63 to > 0 μmol L <sup>-1</sup>	- 4.4	0.1	0	0*/0.4	<0.1	<0.1	4.36 : <0.1 >98 % : <2 %
<i>hypoxic-anoxic</i> 142-167 m, bottom water oxygen conc. 63-0 μmol L <sup>-1</sup>	-1.3	0	0	0*/0.2	<0.1	<0.1	1.3 : <0.1 >92 % : < 8%
<i>anoxic-sulfidic zone</i> >167 m, sulfide present in anoxic bottom water	0	0	0	0.5/3.7	0.1	1.1	0: 1.1** 0 % : 100 %

Negative numbers denote downward flux, positive numbers upward flux

\* bottom water sulfide was zero

\*\* potential oxygen demand is higher than oxygen availability, thus reducing components are emitted



1 Table 4. Oxygen consumption in hypoxic areas of the Black Sea, n.d. = not determined.

2

Area	Water depth (m)	Oxygen concentration ( $\mu\text{mol L}^{-1}$ )	TOU ( $\text{mmol m}^{-2} \text{d}^{-1}$ )	DOU ( $\text{mmol m}^{-2} \text{d}^{-1}$ )	Method	Fauna	Reference
Bay of Varna	24	230	33.3		in situ chamber	living organisms	
Danube delta front	26	160	25.9		(TOU)	living organisms	
Danube prodelta	27	0				living organisms	Fridel et al. 1998
shelf edge	134	40	0			no living organisms	
shelf edge	142	30	5.7			living organisms	
Romanian Shelf	62	211	39.8	11.9	in situ chamber	<i>Mytilus galloprovinciales</i>	Wenzhöfer et al. 2002
	77	213	11.1	5.8	(TOU)/	<i>Modiolus phaseolinus</i>	
	100	75	4.3	2.3	microsensors	<i>Modiolus phaseolinus</i>	
	180	8	0	0	(DOU)	<i>no macrofauna</i>	
NW Shelf	52	285	13.5, 10, 11.6		ex situ core	n.d.	Wijsman et al. 2001
	54	314	11, 6.1		incubations		
	57	243	3.7		(TOU)		
	72	284					
	120	126					
	137	190					
Crimean Shelf	135	95	4.2-6		Eddy correlation		Holtappels et al., 2013
Crimean Shelf	104	110-134	11.6	4.6	in situ chamber	living organisms	this study
	135	18-149	6.7	4.4	(TOU)/	living organisms	
	155	19-11	n.d.	1.3	microsensors (DOU)	living organisms, including fish	

3 Fig. 1: Sediment sampling locations (TVMUC = video-guided multicorer, PUC = JAGO pushcores) and deployment sites of benthic chamber  
4 and microprofiler with MOVE and lander (KAMM) along the transect from shallower (101 m) to deeper (207 m) water depth. Inset: working  
5 area on the outer Western Crimean Shelf (red square) in the Black Sea.

6 Fig. 2: Synthesis of oxygen concentrations in bottom water (circles) measured during the 2 weeks of the cruise (n=85). For continuously  
7 measuring instruments (BBL profiler, optode on JAGO, benthic lander, moorings) only an average value per deployment, dive or day was  
8 included. Maximum depth above the sediment was 12 m (CTD), minimum depth above the sediment was about 5 cm (Clark-type oxygen  
9 microelectrodes). Additionally, sulfide distribution in bottom waters during the same sampling period are shown (white diamonds, n=43). From  
10 depth distribution of oxygen and sulfide the distribution in i) oxic, ii) oxic-hypoxic, iii) hypoxic-anoxic and iv) anoxic-sulfidic zone was deduced.

11 Fig. 3: Abundance of meiobenthos in the upper five centimeter of the sediment under different oxygen regimes. The middle line in each box  
12 depicts the median, while both whiskers and outliers indicate the distribution of remaining data points.

13 Fig. 4: Cluster dendrogram of meiofauna abundances for different station depths based on the inverse of Bray-Curtis dissimilarity.

14 Fig. 5: Examples of high-resolution oxygen profiles under different oxygen regimes. Differences in bottom water oxygen concentrations  
15 (reflected in profile shape and oxygen penetration depth) are clearly visible between sites and deployments.

16 Fig. 6: Examples of individual oxygen profiles measured in the sediment (white circles) and modeled with PROFILER (black lines). Volumetric  
17 rates are combined in discrete layers (dashed line) and exhibit different depths and degrees of oxygen consumption rates in different zones and  
18 under different bottom water oxygenation.

19 Fig. 7: Distribution of reduced pore water species and oxidized and solid phase iron and sulfur species along the depth transect in the upper 30  
20 cm of the sediment (symbols with dotted lines). Solid lines are the model results and dashed lines represent production and consumption rates.

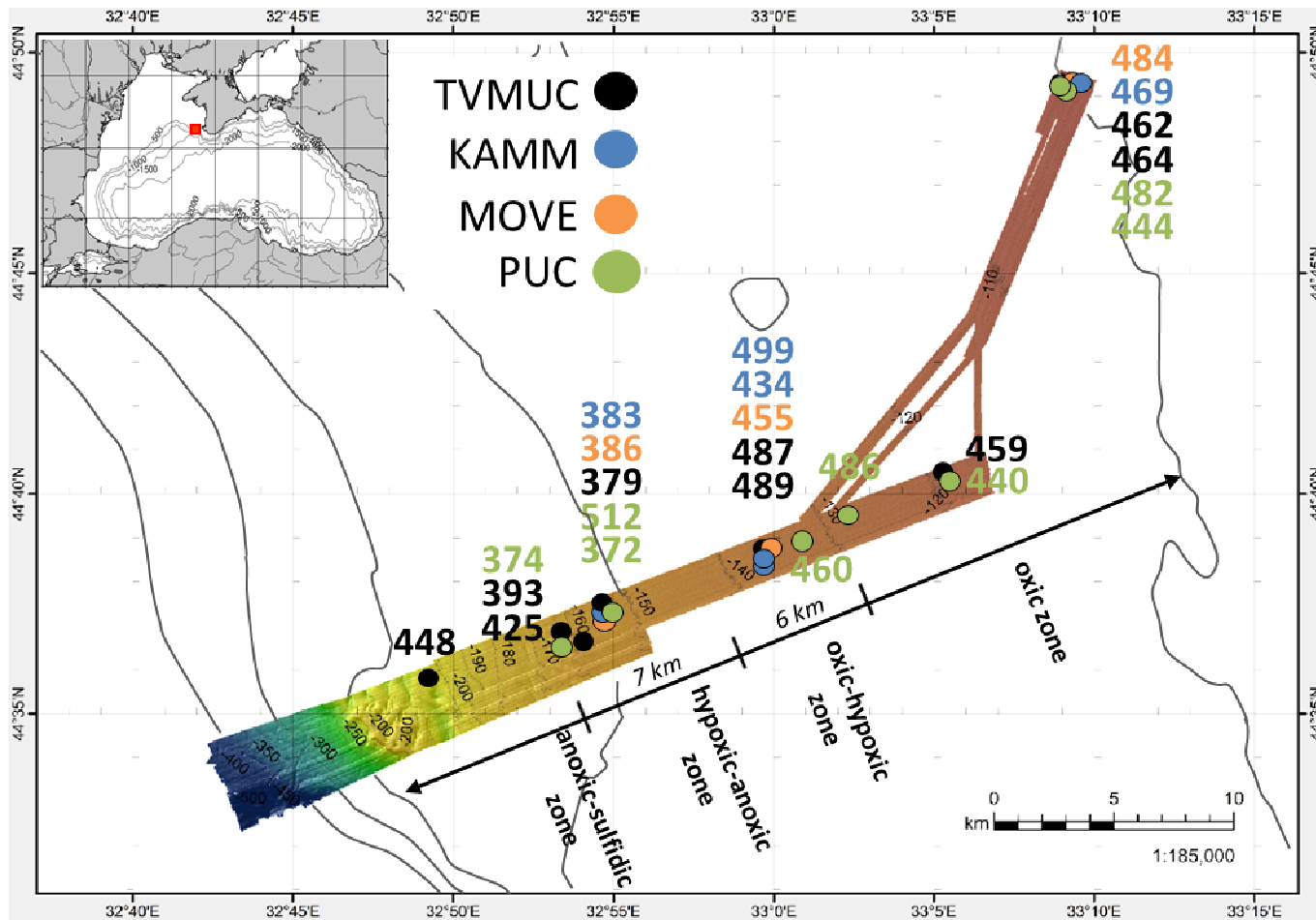


Figure 2

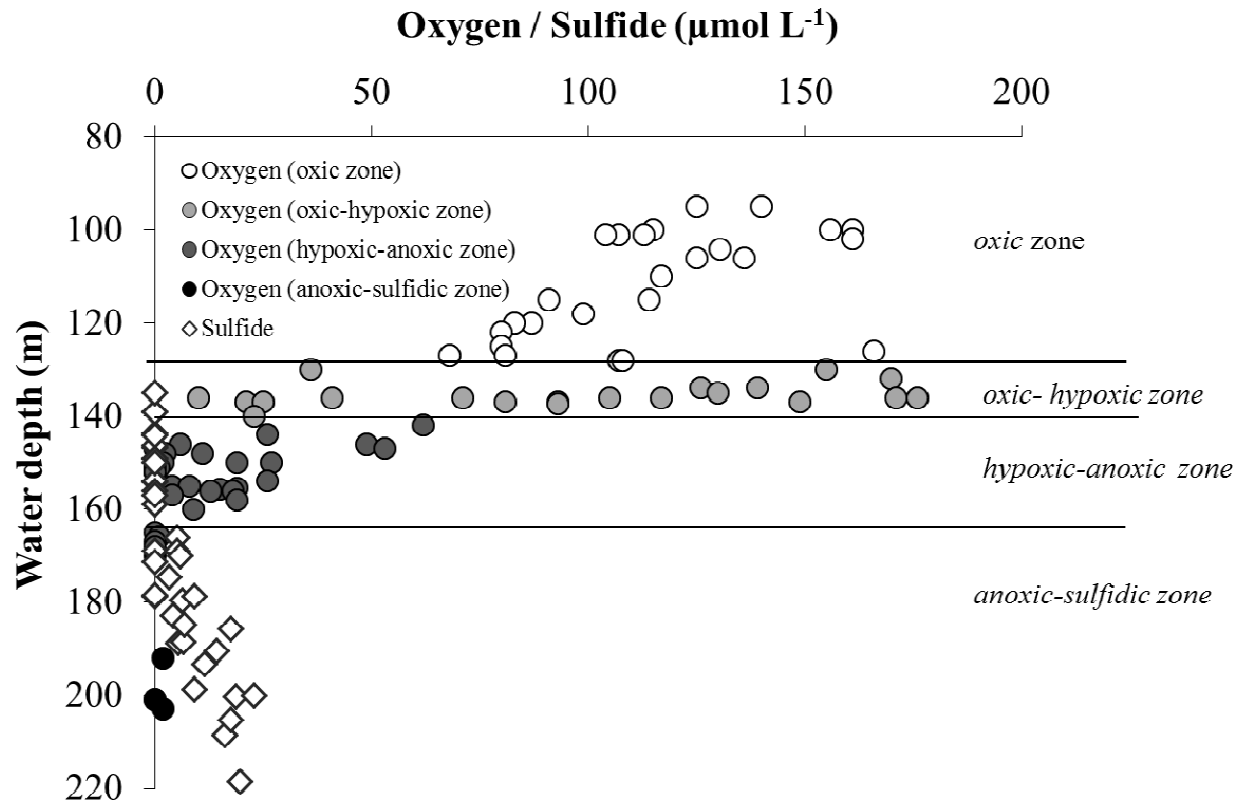


Figure 2

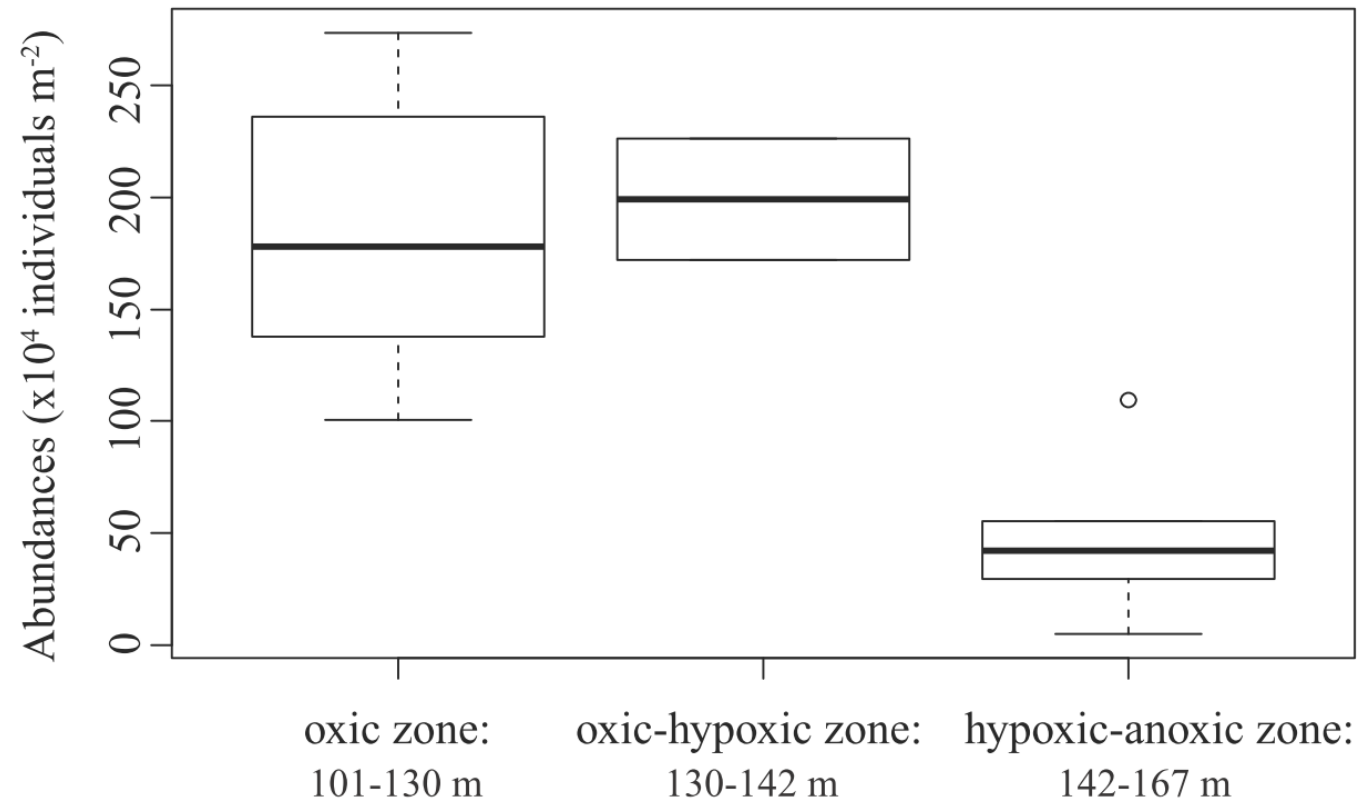


Figure 3

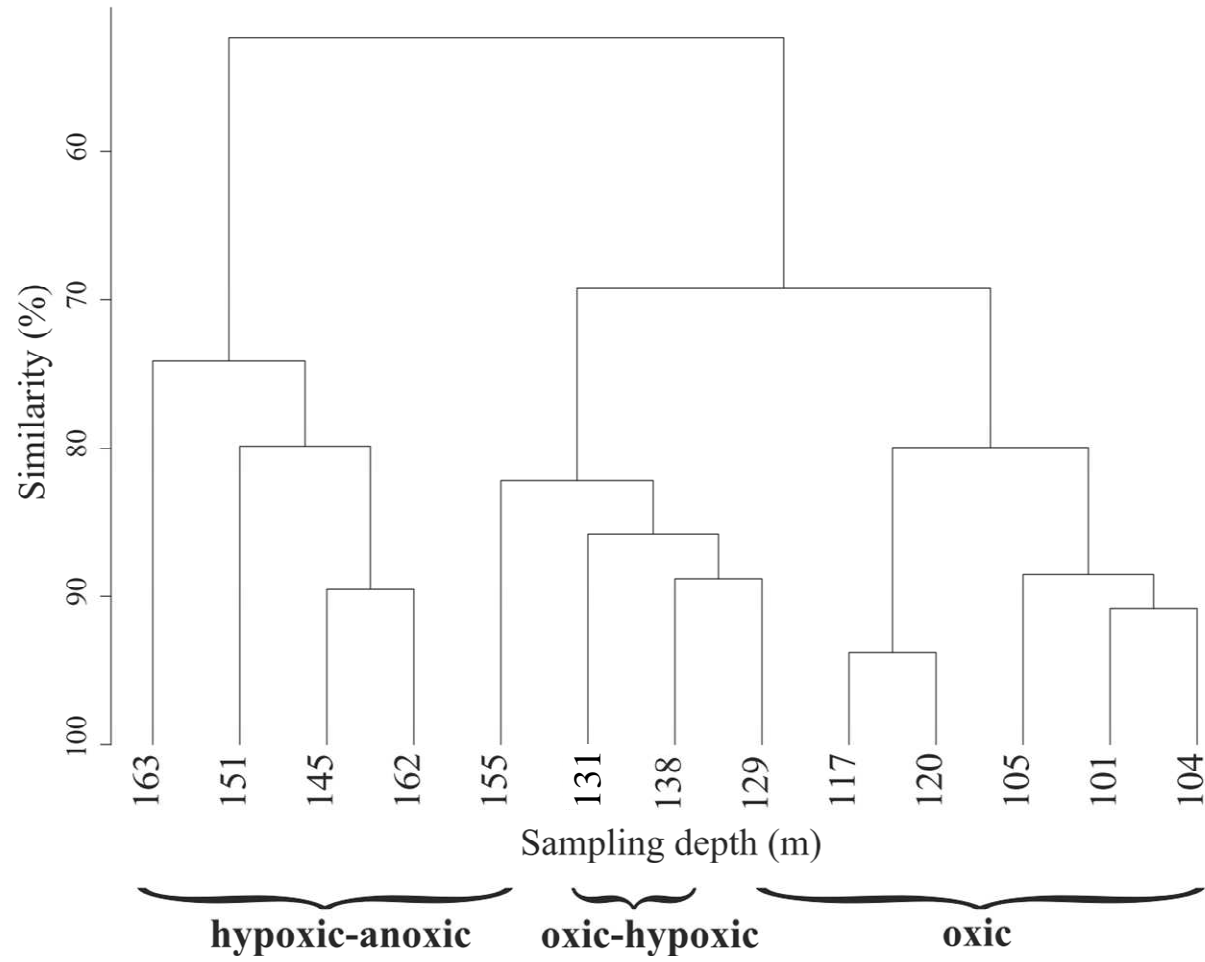
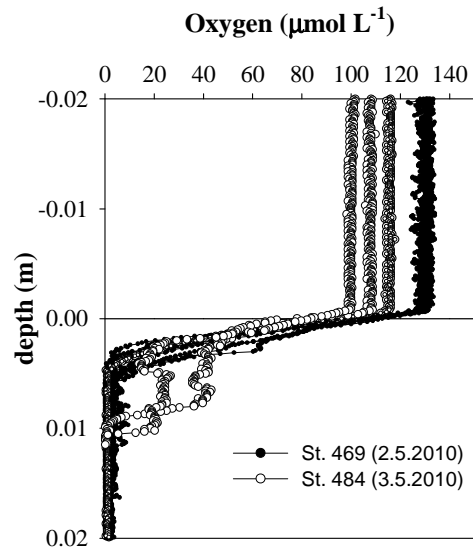
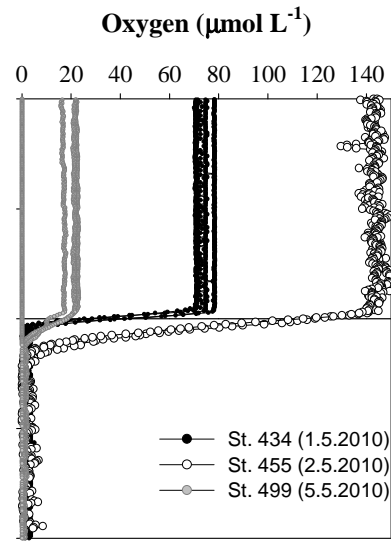


Figure 4

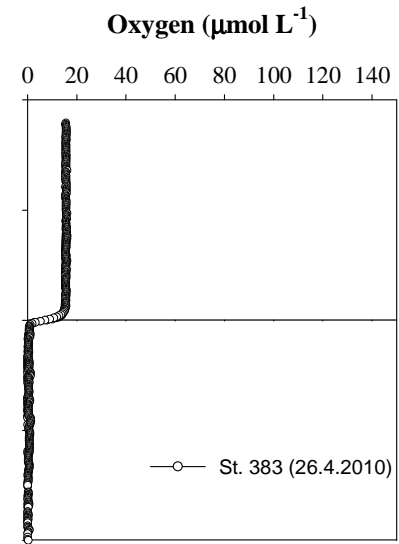




**a) oxic zone**



**c) oxic-hypoxic zone**



**e) hypoxic-anoxic zone**

Figure 5

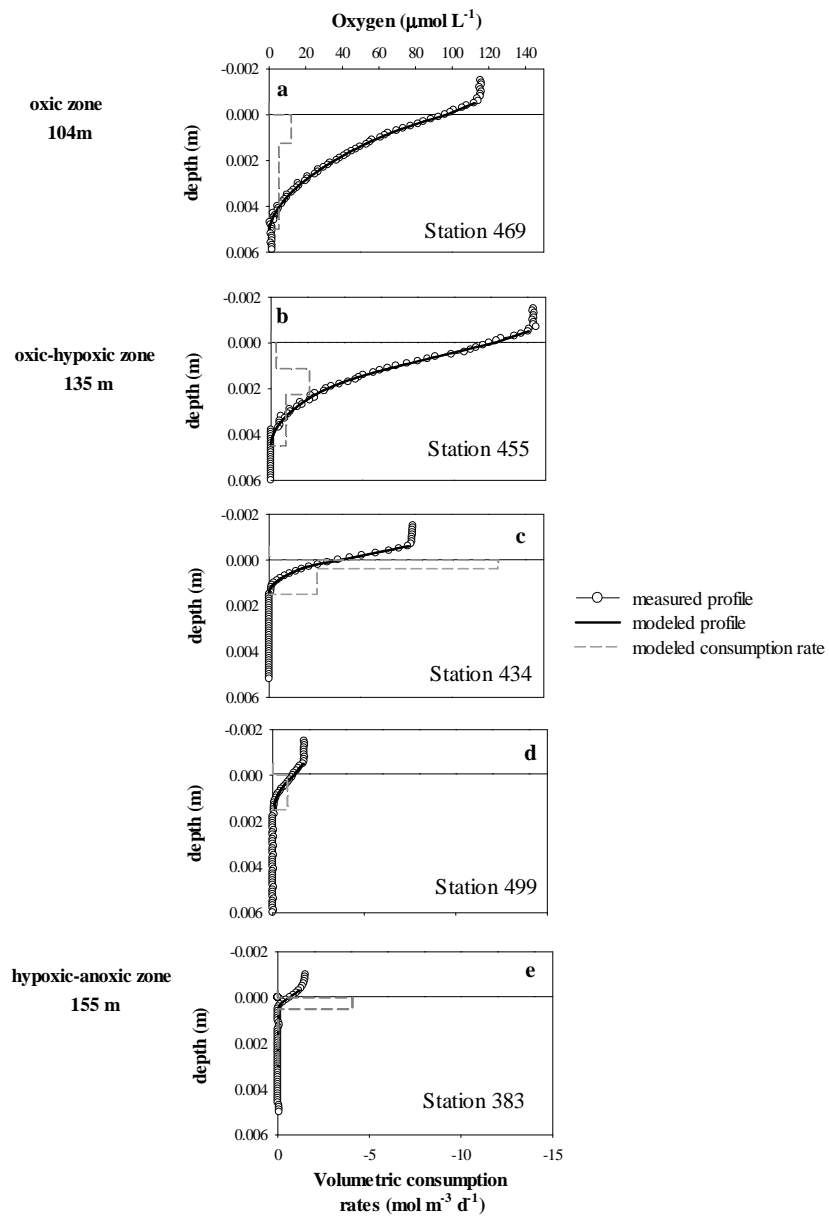


Figure 6

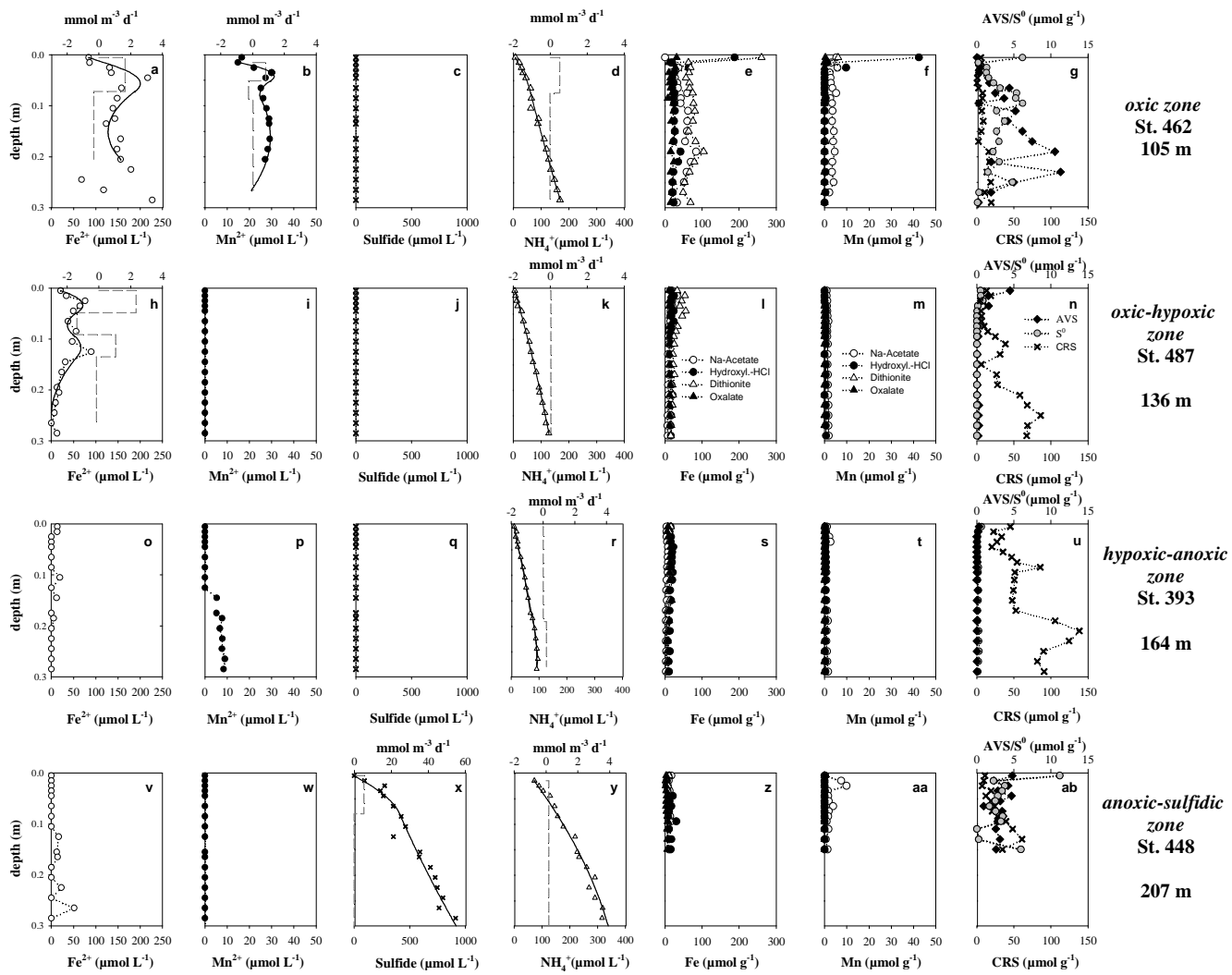


Figure 7